

Molecular and Cellular Biology



ISSN: (Print) (Online) Journal homepage: www.tandfonline.com/journals/tmcb20

MANCR IncRNA Modulates Cell-Cycle Progression and Metastasis by Cis-Regulation of Nuclear *Rho-GEF*

Deepak K. Singh, Zhengmin Cong, You Jin Song, Minxue Liu, Ritu Chaudhary, Dazhen Liu, Yu Wang, Rishabh Prasanth, Rajendra K C, Simon Lizarazo, Miriam Akhnoukh, Omid Gholamalamdari, Anurupa Moitra, Lisa M. Jenkins, Rohit Bhargava, Erik R. Nelson, Kevin Van Bortle, Supriya G. Prasanth & Kannanganattu V. Prasanth

To cite this article: Deepak K. Singh, Zhengmin Cong, You Jin Song, Minxue Liu, Ritu Chaudhary, Dazhen Liu, Yu Wang, Rishabh Prasanth, Rajendra K C, Simon Lizarazo, Miriam Akhnoukh, Omid Gholamalamdari, Anurupa Moitra, Lisa M. Jenkins, Rohit Bhargava, Erik R. Nelson, Kevin Van Bortle, Supriya G. Prasanth & Kannanganattu V. Prasanth (2024) MANCR IncRNA Modulates Cell-Cycle Progression and Metastasis by Cis-Regulation of Nuclear *Rho-GEF*, Molecular and Cellular Biology, 44:9, 372-390, DOI: 10.1080/10985549.2024.2383773

To link to this article: https://doi.org/10.1080/10985549.2024.2383773

+	View supplementary material 🗗
	Published online: 12 Aug 2024.
	Submit your article to this journal $oldsymbol{\mathcal{C}}$
ılıl	Article views: 71
a`	View related articles 🗹
CrossMark	View Crossmark data 🗹





MANCR IncRNA Modulates Cell-Cycle Progression and Metastasis by Cis-Regulation of Nuclear *Rho-GEF*

Deepak K. Singh^{a*‡}, Zhengmin Cong^{a*}, You Jin Song^{a*}, Minxue Liu^a, Ritu Chaudhary^b, Dazhen Liu^a, Yu Wang^c, Rishabh Prasanth^d, Rajendra K C^e, Simon Lizarazo^c, Miriam Akhnoukh^a, Omid Gholamalamdari^a, Anurupa Moitra^a, Lisa M. Jenkins^f, Rohit Bhargava^{g,h}, Erik R. Nelson^{c,h,i,j,k}, Kevin Van Bortle^a, Supriya G. Prasanth^{a,h} , and Kannanganattu V. Prasanth^{a,h}

^aDepartment of Cell and Developmental Biology, University of Illinois at Urbana-Champaign, Urbana, Illinois, USA; ^bDepartment of Head and Neck-Endocrine Oncology, H. Lee Moffitt Cancer Center and Research Institute, Tampa, Florida, USA; ^cDepartment of Molecular and Integrative Physiology, University of Illinois at Urbana-Champaign, Urbana, Illinois, USA; ^dUniversity Laboratory High School, Urbana, Illinois, USA; ^eCenter for Biophysics and Quantitative Biology, University of Illinois at Urbana-Champaign, Urbana, Illinois, USA; ^fLaboratory of Cell Biology, Center for Cancer Research, National Cancer Institute, NIH, Bethesda, Maryland, USA; ^gDepartment of Bioengineering, Cancer Center at Illinois, Beckman Institute of Advanced Science and Technology, UIUC, Urbana, Illinois, USA; ^hCancer Center at Illinois, USA; ^hBeckman Institute for Advanced Science and Technology, University of Illinois at Urbana-Champaign, Urbana, Illinois, USA; ^lCarl R. Woese Institute for Genomic Biology-Anticancer Discovery from Pets to People, University of Illinois at Urbana-Champaign, Urbana, Illinois, USA; ^kDivision of Nutritional Sciences, University of Illinois at Urbana-Champaign, Urbana, Illinois, USA; ^kDivision of Nutritional Sciences, University of Illinois at Urbana-Champaign, Urbana, Illinois, USA; ^kDivision of Nutritional Sciences, University of Illinois at Urbana-Champaign, Urbana, Illinois, USA; ^kDivision of Nutritional Sciences, University of Illinois at Urbana-Champaign, Urbana, Illinois, USA; ^kDivision of Nutritional Sciences, University of Illinois at Urbana-Champaign, Urbana, Illinois, USA; ^kDivision of Nutritional Sciences, University of Illinois at Urbana-Champaign, Urbana, Illinois, USA; ^kDivision of Nutritional Sciences, University of Illinois at Urbana-Champaign, Urbana, Illinois, USA; ^kDivision of Nutritional Sciences, University of Illinois at Urbana-Champaign, Urbana, Illinois, USA; ^kDivision of Nutritional Sciences, University of Illinois at Urbana-Champaign, Urbana, Illinois

ABSTRACT

A significant number of the genetic alterations observed in cancer patients lie within nonprotein-coding segments of the genome, including regions coding for long noncoding RNAs (IncRNAs). LncRNAs display aberrant expression in breast cancer (BrCa), but the functional implications of this altered expression remain to be elucidated. By performing transcriptome screen in a triple negative BrCa (TNBC) isogenic 2D and 3D spheroid model, we observed aberrant expression of >1000 IncRNAs during BrCa progression. The chromatin-associated IncRNA MANCR shows elevated expression in metastatic TNBC. MANCR is upregulated in response to cellular stress and modulates DNA repair and cell proliferation. MANCR promotes metastasis as MANCR-depleted cells show reduced cell migration, invasion, and wound healing in vitro, and reduced metastatic lung colonization in xenograft experiments in vivo. Transcriptome analyses reveal that MANCR modulates expression and pre-mRNA splicing of genes, controlling DNA repair and checkpoint response. MANCR promotes the transcription of NET1A, a Rho-GEF that regulates DNA damage checkpoint and metastatic processes in *cis*, by differential promoter usage. Experiments suggest that MANCR regulates the expression of cancer-associated genes by modulating the association of various transcription factors and RNA-binding proteins. Our results identified the metastasis-promoting activities of MANCR in TNBC by *cis*-regulation of gene expression.

ARTICLE HISTORY

Received 21 March 2024 Revised 8 July 2024 Accepted 12 July 2024

KEYWORDS

IncRNA; cell cycle; NET1; hnRNP L; breast cancer

Introduction

Breast cancer (BrCa) ranks as the second most prevalent cancer among women in the United States and stands as a significant contributor to mortality worldwide. BrCa is a heterogenous disease, which is categorized into various molecular sub-types.¹ Each subtype exhibits unique clinical behaviors, distinct therapeutic responses, and varying expressions of receptors, including estrogen receptor (ER), progesterone receptor (PR), and human epidermal growth factor 2 (HER2) receptor. BrCa is classified into various molecular subtypes: luminal A (ER-positive and PR-positive, HER2-negative), luminal B (ER-positive and PR-positive and HER2-positive or negative), HER2-positive (ER – ve, PR – ve, HER2 +ve), and triple negative BrCa (TNBC: ER/PR/HER2 negative).¹ TNBC

presents the worst clinical outcome due to poor response to hormone-targeted therapies, disease heterogeneity, and chemotherapy resistance. Thus, there is an urgent need to understand the biology of TNBC to identify suitable prognostic and diagnostic markers.

Gene expression studies in BrCa patient samples reported differential expression of a significant number of genes, controlling key cellular pathways during cancer progression and metastasis. Mechanistic studies revealed that such genes contribute to the disease phenotype. Approximately 2% of the human genome is dedicated to protein-coding sequences, while a significant portion, around 70–80%, is transcribed into noncoding transcripts.² Interestingly, most germline mutations associated with susceptibility to cancers are found

CONTACT Kannanganattu V. Prasanth kumarp@illinois.edu

*Co-first authors.

[‡]Present Address: Department of Cell Biology, Albert Einstein College of Medicine, New York, USA.

in noncoding regions of the genome, including gene regulatory elements, as well as within noncoding RNA (ncRNA) genes.^{3,4} Long noncoding RNAs, ncRNAs of > 300 nucleotides in length, comprise the least studied but most complex group of ncRNAs.⁵ The IncRNAs engage in diverse functions, show differential abundance, interact with different subsets of proteins, and regulate their activity.⁵ The human genome is estimated to code for > 19,000 lncRNA genes (https:// www.gencodegenes.org). A significant number of these IncRNAs show altered expression in BrCa patient samples and are associated with specific BrCa properties such as chemoresistance.⁶ However, very little is known about the molecular function of lncRNAs and their involvement in BrCa progression and metastasis. Mechanistic studies on a handful of IncRNAs reveal they play central roles in BrCa disease pathology. For example, the oncogenic IncRNA, HOTAIR, represses the expression of protein-coding genes by modulating the epigenetic landscape. We and others have demonstrated that MALAT1 IncRNA regulates BrCa progression and metastasis by modulating transcription and RNA processing.⁹ The natural antisense IncRNA, PDCD4-AS1, prevents TNBC progression by enhancing the expression of the tumor suppressor PDCD4.¹⁰ Furthermore, Inc02095 promotes TNBC progression by enhancing the expression of the oncogenic transcription factor, Sox9. 11 Finally, studies from the Spector laboratory demonstrated key roles played by several lncRNAs, such as MaTARs, in BrCa progression and metastasis. 12,13

Simple "petri-dish"-based monolayer 2D cell cultures persist as the predominant in vitro model for comprehending cancer cell biology, owing to their superior accessibility, costeffectiveness, and user-friendly nature, notwithstanding acknowledged limitations. 14,15 Over the last decade, several 3D (spheroid and organoid) cell culture models have been developed, which better recapitulate the complexity observed under physiological conditions compared to 2D cultures. 16,17 Spheroids are 3D structures formed typically of one cell type, aggregating, and growing together. Studies using several spheroid tumor models revealed that they better reproduce tumor properties, such as heterogeneous cellular architecture, cellular signaling, establishment of gradients of metabolites, nutrients within the tumor, 16-18 resistance to chemotherapy and tumor-specific gene expression. Thus, comparing 2D and 3D cultures may provide unique vulnerabilities for therapeutic targeting.

Breast carcinoma progresses by sequential genetic modifications of benign hyperplasia of mammary duct epithelial cells. This ultimately develops into invasive tumors, which metastasize into distant organs. To comprehend the biology of IncRNAs during BrCa progression, we performed deeptranscriptome analyses on an established isogenic mammary epithelial cell-line-derived TNBC progression model system. RNA-seg analyses from cells grown under 2D, and 3D spheroids identified a sub-set of lncRNAs whose aberrant expression were associated with TNBC and metastasis. Further, studies on one such IncRNA, LINC00704 or MANCR (mitotically associated lncRNA), revealed its involvement in cell cycle progression and metastasis. Several earlier studies reported elevated MANCR levels in TNBC patient and cell lines compared to normal tissues. 19,20 MANCR promoted cancer cell proliferation, including in breast, lung and liver cancers, 20–25 and its expression is linked to genome stability. 20,25,26 However, our results indicate that in TNBC cells, MANCR inhibits cell proliferation, but at the same time promotes cancer cell metastasis. At the mechanistic level, MANCR promotes the transcription of NET1A, a Rho-GEF, and a regulator of DNA damage checkpoint and metastasis, in cis by differential promoter usage. Hence, our findings unearth MANCR's role in promoting metastasis through its regulation of gene expression in cis.

Results

MANCR IncRNA is preferentially upregulated in TNBC

The stages of cancer underlie the manifestation of differential gene expression and downstream signaling pathways. These processes are responsible for the sequential evolution of cancer cells from benign to malignant, enabling further metastasis in different organs. To understand the role of IncRNAs in basal-like/TNBC BrCa progression, we used a well-established isogenic BrCa progression model system described previously.^{27–29} This model system consists of a series of cell lines, namely M1 (nontumorigenic and immortalized MCF10A), M2 (MCF10AT1k.cl2), M3 (MCF10Ca1h), and M4 (MCF10CA1a.cl1) (Figure 1A). M2 cells were generated by stable expression of the oncogenic T24-HRas mutant in M1 cells, followed by xenografting in nude mice. M2 cells are hyperproliferative and form benign hyperplastic lesions, occasionally forming carcinomas in nude mice. M3 (MCF10Ca1h) and M4 (MCF10Ca1a.cl1) cells were derived from the carcinomas arising from the M2 xenografts. Importantly, M3 cells form welldifferentiated low-grade carcinomas with low metastatic potential in nude mice. Conversely, M4 cells generate undifferentiated carcinomas and metastasize into distant organs such as the lungs. Thus, these lines resemble critical steps of basal-like/TNBC progression and metastasis. In addition, the common genetic background reduces the possibility of genetic variation responsible for differential gene expression.¹⁰

Utilizing this model system, we have previously demonstrated the role of several genes in TNBC progression and metastasis.^{8,10,11,29} M1, M2, and M3 cells grown under 3D conditions in Matrigel for 10-14 days formed acini-like structures which, in vivo, morphologically, and phenotypically resemble acini of breast glands (Figure 1A). Due to their highly invasive nature, M4 cells failed to form distinct spheroids after 10-14 days. To identify genes, including IncRNAs, controlling BrCa progression and metastasis, we performed genome-wide transcriptome analyses of cells cultured under 2D and 3D conditions¹⁰ (Supplementary Figure 1Aa and b). Deep RNA-seg analyses (> 200 million reads/sample in biological duplicates) revealed differential expression (0.05 FDR; the absolute value of fold change > 2), of > 3000 genes in the tumorigenic M3 or metastatic M4 cells compared to M1 cells, grown under both 2D (M1 vs M3: 2492 upregulated, 1425 downregulated genes; M1 vs M4: 3353 upregulated, 1928 downregulated genes) (Supplementary Figure 1B and Supplementary Table 1) and 3D conditions (M1 vs M3: 1832

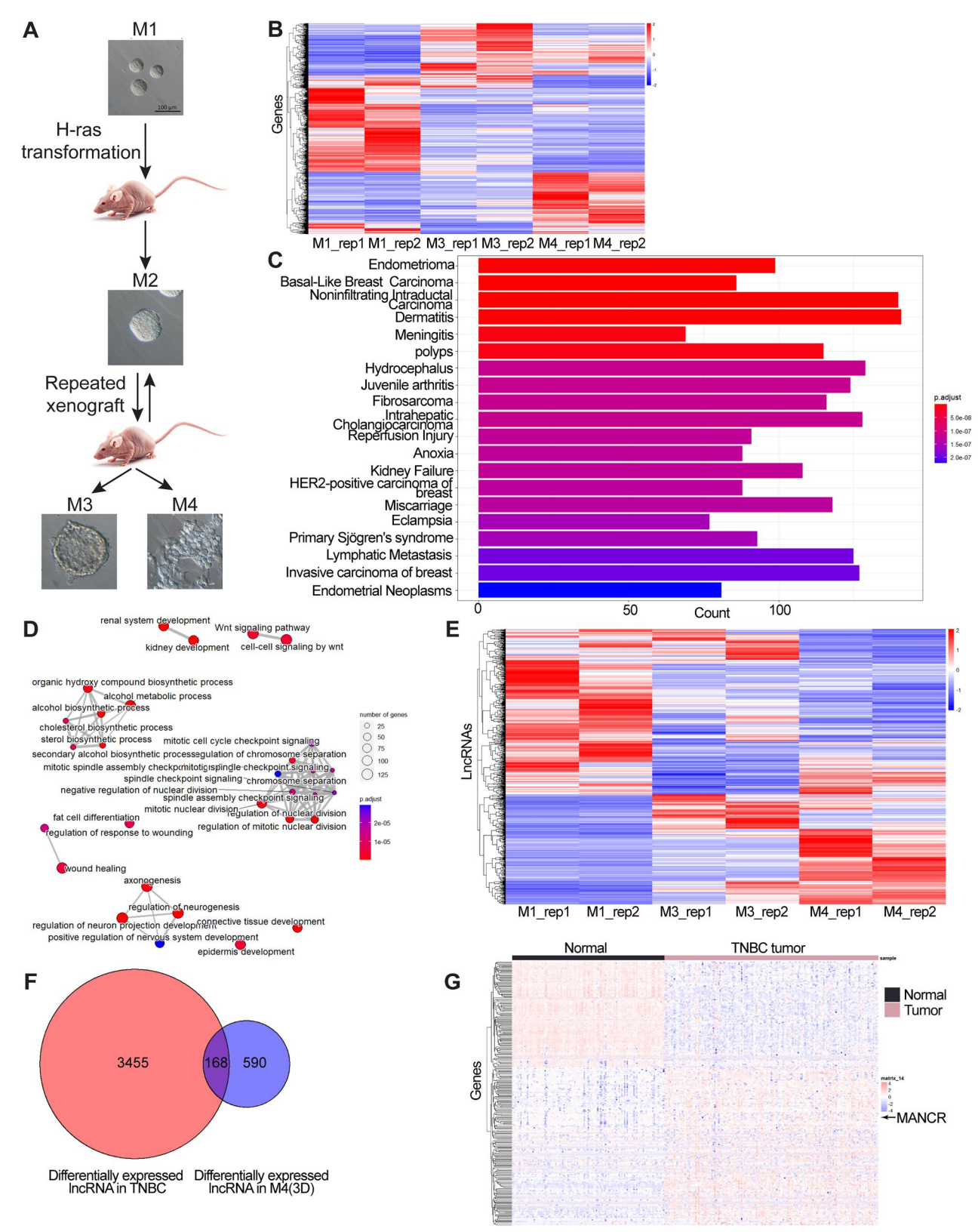


Figure 1. LncRNAs show differential expression in 2D and 3D grown TNBC isogenic cells. (A) Flow chart showing the method of generating M1-M4 cell lines. (B) Heatmap of differentially expressed genes of M1, M3 and M4 in 3D culture identified by RNA-seq. (C) Disease enrichment analysis of differentially expressed genes in M4 (compared to M1) in 3D culture using DisGeNET (http://www.disgenet.org/). (D) Biological process of differentially expressed genes in M4 (compared to M1) in 3D culture identified through gene ontology (GO). (E) Heatmap of differentially expressed lncRNAs of M1, M3 and M4 in 3D culture, identified by RNA-seq. (F) Venn diagram showing the overlap of differentially expressed lncRNAs in TNBC human samples (compared to normal tissue) and M4 (compared to M1 cell line). (G) Heatmap showing the relative expression of M4 up regulated lncRNAs (3D culture) in TNBC tumor tissue samples and adjacent normal tissues. The arrow indicates MANCR relative expression levels in TNBC patient samples.

upregulated, 1515 downregulated genes; M1 vs M4: 2026 upregulated, 2477 downregulated genes) (Figure 1B). We observed a distinct and nonoverlapping subset of genes, which displayed elevated expression in M3 (2D: 832 genes; 3D: 777 genes) or M4 (2D:1693 genes; 3D: 971 genes) cells (Figure 1B, Supplementary Figure 1B and Supplementary Table 1), indicating that these subsets of genes contribute to BrCa progression and metastasis in M3 and M4 cells respectively. To assess the impact of growth conditions on gene expression, we compared the gene expression changes in cells cultured under 2D and 3D conditions. Pertinently, we observed only a small but significant overlap of genes that showed concordant differential expression both under 2D and 3D conditions (M1 vs M3: 932 genes; M1 vs M4: 1295 genes) (Supplementary Figure 1C and D), implying that culture conditions influence gene expression. Moreover, upon conducting gene ontology and disease enrichment analyses on differentially expressed genes in spheroid-cultured M3 or M4 cells, we observed enrichments in several cancer processes, such as basal-like breast carcinoma, noninfiltrating intraductal carcinoma, lymphatic metastasis, and invasive carcinoma of the breast. In addition, cancer-relevant biological processes such as wound healing and mitotic cell-cycle checkpoints were identified as enriched processes (Figure 1C and D; Supplementary Figure 1E and F).

Next, we focused our efforts on identifying IncRNAs exhibiting differential expression under both 2D and 3D grown M3 and M4 cells, compared to nontumorigenic M1 cells. Differential expression of > 1000 lncRNAs was observed (2D: M1 vs M3: 473 upregulated, 328 downregulated; M1 vs M4: 874 upregulated, 295 downregulated) (3D: M1 vs M3: 216 upregulated, 343 downregulated; M1 vs M4: 316 upregulated, 442 downregulated) (Figure 1E and Supplementary Figure 1G). Approximately two hundred IncRNA genes showed concordant changes in expression between 2D and 3D-grown M4 cells compared to M1 (Supplementary Figure 1H). We observed that 168 (of 199) IncRNAs showed concordant differential expression in both M4 cells and TNBC patient samples (Figure 1F), compared to M1 and normal mammary tissues. We observed 98 IncRNAs showed concordant upregulation in M4 cells and human TNBC tumors, whereas 26 of them showed elevated expression only in M4 cells but displayed reduced expression in TNBC patient samples (Figure 1G). Thus, our genome-wide transcriptome analyses using the TNBC mammary epithelial isogenic cancer model system identified hundreds of uncharacterized IncRNAs, which are possibly critical for TNBC progression and metastasis.

MANCR is overexpressed in TNBC

We focused on a candidate intergenic IncRNA, MANCR (LINC00704), which showed elevated expression in both 2D and 3D-grown M4 cells compared to M1. Similarly, MANCR exhibited elevated expression in TNBC patients compared to normal tissues (Figure 1G).^{19,20} MANCR was previously identified as a IncRNA upregulated in basal-like/TNBC BrCa patient samples and cells. 19,20 Earlier studies reported MANCR to promote cell proliferation in several cancer models, including

BrCa, 20-25 and its expression is linked to cell viability and genomic stability. 20,25,26 However, the exact role of MANCR in cancer progression is yet to be determined. MANCR is a multi-exonic transcript (four exons) and is highly expressed in M4 cells compared to M1, M2, and M3 cell lines (Figure 2A). RT-qPCR data exhibited a progressive elevation in MANCR RNA levels from M1 to M4, demonstrating an 80-fold increase in MANCR levels in M4 compared to M1 (Figure 2B). In general, basal-like/TNBC BrCa cell lines (M2, M3, M4, Hs578T, BT549, MDA-MB-231 & MDA-MB-468) show elevated MANCR levels compared to BrCa cells from luminal and HER2+ve subtypes (Supplementary Figure 2A). In addition, body map data from UCSC showed elevated levels of MANCR in organs such as the breast and spleen (Supplementary Figure 2B). RTqPCR also confirmed elevated levels of MANCR in spleen and breast tissues (Supplementary Figure 2C). Northern blotting revealed MANCR to be a ~1.6 kb transcript in TNBC cells (Figure 2C). PhyloCSF, CPAT and Bazzini small ORFs algorithm predicted MANCR as a IncRNA (Supplementary Figure 2Da to c). Cell fractionation analyses revealed that \sim 80% of MANCR localized in the nucleus where it predominantly associated with the chromatin (Figure 2D and Supplementary Figure 2E). LncATLAS data demonstrated nuclear localization of MANCR in multiple cell lines (Supplementary Figure 2F). Furthermore, single molecule fluorescent RNA in-situ hybridization (smFISH) in M4 and MDA-MB-231 interphase cells revealed MANCR to be predominantly localized in the nucleus. In addition, a significant fraction of MANCR was also distributed in the cytoplasm (Figure 1E and Supplementary Figure 2G). An earlier study reported MANCR to be enriched in the mitotic chromosomes in MDA-MB-231 cells. Hence, the gene was named as Mitotically associated IncRNA (MANCR)²⁰. However, we did not see any enrichment of MANCR on the mitotic chromosomes of both M4 and MDA-MB-231 (Supplementary Figure 2H). Few of the MANCR + ve foci in mitotic cells, in fact, localized in the cytoplasm surrounding the chromosomes. As observed by an RNA stability assay, MANCR is a stable transcript with a half-life of ~4 h (Figure 2F). M4 cells contain \sim 230 copies of MANCR (Supplementary Figure 21).

Aggressive BrCa subtypes, such as TNBC/basal-like BrCa, are characterized by higher levels of genomic instability. 30,31 We tested whether MANCR levels are influenced by various cellular stress, such as DNA damage and hypoxia. We observed a significant increase in the levels of MANCR in M1 and M4 cells treated with DNA damaging agent, hydroxyurea (HU), which depletes the cellular dNTPs pool by inhibiting ribonucleoside diphosphate reductase (Figure 2G and Supplementary Figure 2Ja). HU treatment for 24h induces double-strand DNA breaks (DSBs) due to collapsed replication forks, and activates the cell-cycle checkpoint, as observed by increased levels of p21 and yH2AX (Supplementary Figure 2Jb to d). Surprisingly, MANCR-induced in response to DNA damage in nontumorigenic M1 cells, were enriched in the cytoplasm as observed by smFISH (Supplementary Figure 2K). Mammary epithelial cells also showed enhanced expression of MANCR in response to hypoxia treatment (0.2% O₂ for 24 h) (Figure 2H). Our results show that MANCR is a chromatin-associated, stable IncRNA, which is highly expressed in

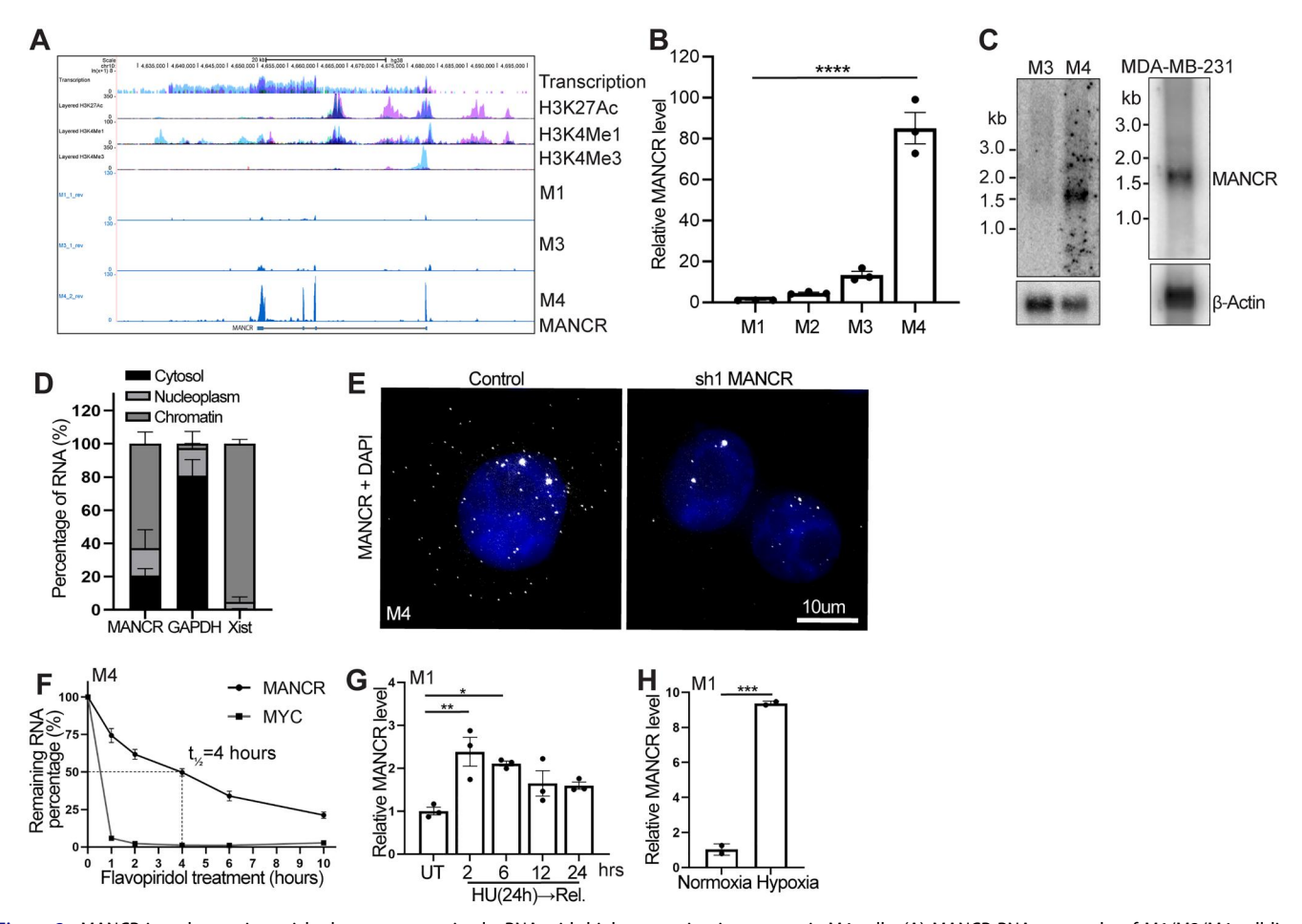


Figure 2. MANCR is a chromatin-enriched stress-responsive lncRNA with high expression in metastatic M4 cells. (A) MANCR RNA-seq peaks of M1/M3/M4 cell lines, transcription status and histone marker tracks (H3K4me1, H3K4me3, and H3K27ac) in various ENCODE cell lines shown in the UCSC genome browser. (B) MANCR levels in M1–M4 cell lines measured by RT-qPCR. (C) MANCR expression in M3, M4, and MDA-MB-231 cell lines detected by Northern blot. (D) Relative percentage of MANCR, GAPDH, and XIST lncRNA in M4 cytosol/nucleoplasm/chromatin fractions measured by RT-qPCR. (E) M4 MANCR localization in M4 wild-type and MANCR-depleted cells detected by single-molecule RNA-FISH (smRNA-FISH). DNA is counterstained with DAPI. Scale bar: 10 μ m. (F) Half-life of MANCR in M4 cells measured by flavopiridol (1 M) treatment followed by RT-qPCR. Myc was used as a control with an already known half-life of 30 min. (G and H) Increased MANCR RNA level upon HU treatment (24 h) and release (G) and upon hypoxia (0.2% O_2 , 24 h) (H) in M1 cell line measured by RT-qPCR. Data were presented as mean \pm SD. Statistical analysis was conducted using unpaired two-tailed t tests. Significance levels were denoted as follows: *P < 0.05, **P < 0.01, ***P < 0.001, ****P < 0.0001. The same statistical approach was applied consistently across all panels if not specified.

metastatic TNBC cells and induced in response to various cellular stress.

MANCR regulates cell proliferation and DNA damage response

Since MANCR overexpression in basal-like/TNBC patients is correlated with poor survival rate of patients,²⁰ it is vital to investigate its role in cancer progression and metastasis. To this end, we generated a MANCR stable knockdown M4 cell line by using two different shRNAs targeting separate exons (Supplementary Figure 3A; sh1 and sh2). We observed 90% and 55% KD efficiency with shRNA1 (sh1) and shRNA2 (sh2), respectively, in M4 cells (Figure 3A). We also successfully depleted MANCR in M4 cells using CRISPRi-approach, in which cells stably expressing guide-RNA (targeting the promoter of *MANCR*) and dCas9-KRAB (ZIM3)³² reduced MANCR levels (Figure 3A). In contrary to what was reported earlier, the knockdown of MANCR in M4 cells, by both using shRNA and CRISPRi, led to a significant increase in long-term cell proliferation as observed by anchorage-dependent plastic

colony formation assay for 14 days (Figure 3Ba and b and Supplementary Figure 3B). We then performed a rescue assay in which MANCR was stably induced under the control of doxycycline (DOX) in M4 cells lacking endogenous MANCR. MANCR-depleted cells overexpressing exogenous MANCR successfully rescued the hyperproliferation phenotype (Figure 3C). Further, short-term cell proliferation assay (75–100 h) revealed that MANCR-depletion enhanced M4 cell proliferation (Figure 3D). In contrast, stable overexpression of MANCR in M4 cells dramatically inhibited cell proliferation (Figure 3D). Finally, overexpression of MANCR in the M1 cells also reduced cell proliferation (Figure 3E and Supplementary Figure 3Ca and b). Our results suggest that MANCR plays a principal role in inhibiting cell proliferation. This contradicts results from a previous study, where the authors reported that the transient knock down of MANCR using LNA-modified antisense oligonucleotides in MDA-MB-231 cells reduced cell proliferation.²⁰ We stably depleted MANCR in two other TNBC cell lines, including MDA-MB-231, and MDA-MB-468 and determined the effect on cell proliferation. Similar to M4 cells, MANCR-depleted MDA-MB-231 and MDA-MB-468 cells

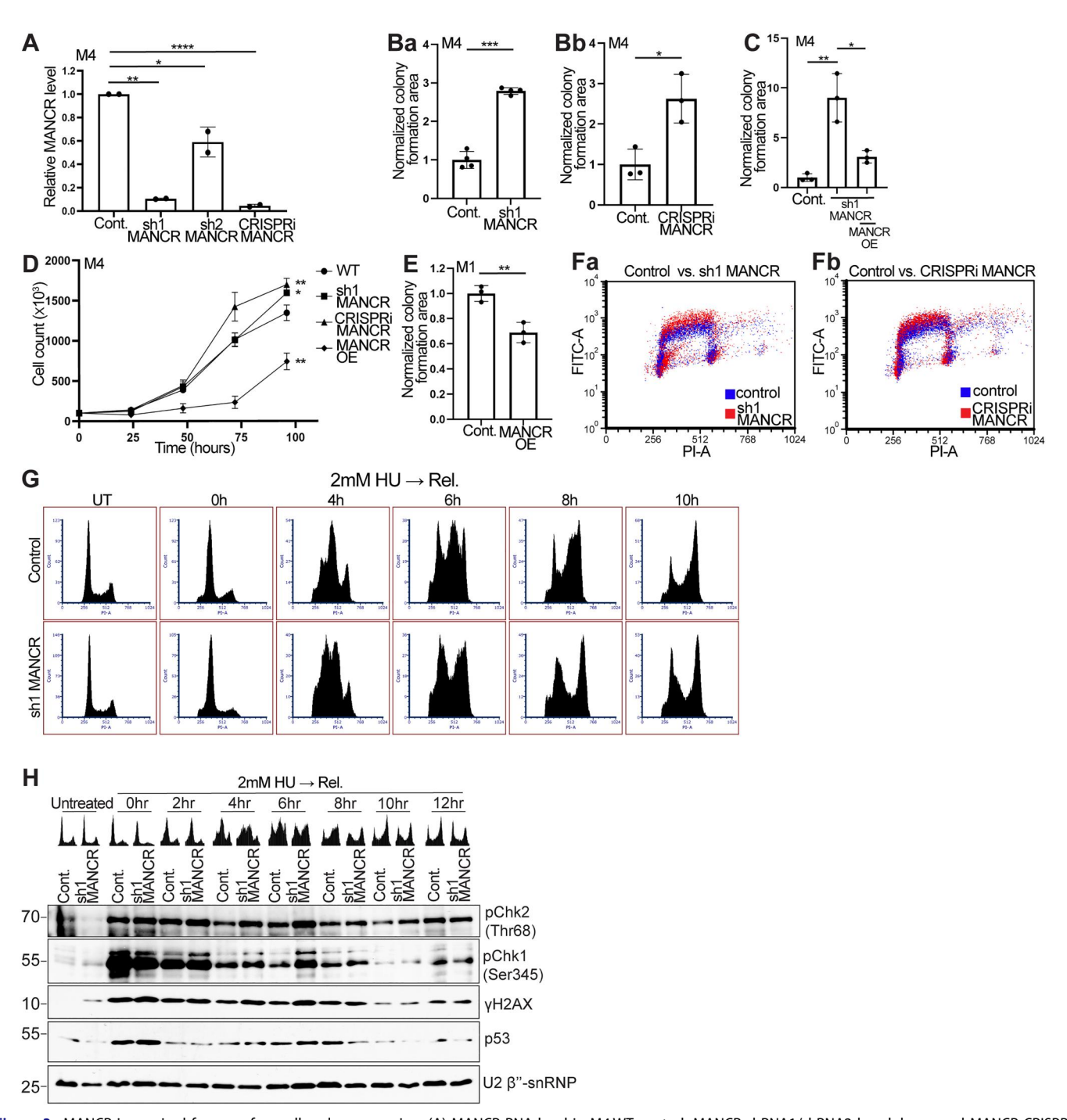


Figure 3. MANCR is required for error-free cell cycle progression. (A) MANCR RNA level in M4 WT control, MANCR shRNA1/shRNA2 knockdown, and MANCR CRISPRi cell lines measured by RT-qPCR. (B) Long-term proliferation of M4 WT (control), MANCR shRNA1 knockdown (Ba) and MANCR CRISPRi (Bb) cells measured by anchorage-dependent colony formation assay. (C) Long-term proliferation of WT (control), MANCR-depleted, and MANCR-rescued M4 cells measured by anchoragedependent colony formation assay. (D) Proliferation curve of M4 WT, MANCR-depleted, and MANCR overexpressed M4 cells. Unpaired two-tail t tests were performed at the last time point. (E) Long-term proliferation of WT and MANCR overexpressed M1 cells measured by anchorage-dependent colony formation assay. (F) BrdU-PI-flow cytometry analyses in WT, shRNA1- (Fa) and CRISPRi-treated (Fb) M4 cells. 8000 cells from each sample are shown in scatter plots. (G) Cell cycle profiles of M4 WT/MANCR shRNA1-treated M4 cells measured by flow cytometry after 24 h 2 mM HU treatment and release for indicated time points (0 h-10 h). H. The expression of proteins involved in cell cycle check point and DNA damage response after HU treatment in M4 WT/MANCR shRNA1-treated cells measured by Western blot. Data were presented as mean \pm SD. Statistical analysis was conducted using unpaired two-tailed t tests. Significance levels were denoted as follows: *P < 0.05, **P < 0.01, ***P < 0.001, ****P < 0.0001.

showed increased cell proliferation (Supplementary Figures 3Da to c and 3Ea to c). Finally, we tested the involvement of MANCR in in vivo tumor formation by orthotopically transplanting control and MANCR-depleted M4 cells into the mammary fat pads of nude mice and recorded the effect on tumor progression. Mice transplanted with MANCR-depleted

M4 cells showed a significant increase in tumor size, further supporting the model that MANCR negatively regulates cell proliferation and tumor progression (Supplementary Figure 3F).

Given that cellular stress, such as DNA damage or hypoxia, induces MANCR levels and that MANCR levels impact cell proliferation, we examined MANCR's role in cell cycle progression. BrdU-PI flow cytometry analyses revealed that MANCR-depleted M4 cells showed increased BrdU incorporation, implying that more origins are firing, which leads to a faster S-phase progression (Figure 3Fa and b). Next, we treated control and MANCR-depleted M4 cells with 2 mM HU for 24 h to arrest them at the G1/S transition of the cell cycle. Control and MANCR-depleted cells released from HU arrest and release were checked for cell cycle progression using flow cytometry analyses. Compared to control M4 cells, MANCR-depleted cells post-HU arrest and release showed an increased population of cells stuck at the G1/S boundary and within S-phase (Figure 3G; see 4-8h). Slowed/defective Sphase progression in cells released after DNA damage could be due to inefficient repair, leading to activated cell cycle checkpoint. Therefore, we assessed the levels of cell cycle checkpoint marker proteins in control and MANCR-depleted cells during post-DNA damage recovery. Immunoblot analyses showed the induction of known checkpoint proteins such as pChk2, pChk1, yH2AX, and p53 in both control and MANCR KD cells upon HU (0 h release) treatment and during initial stages of release (2 h post-release) (Figure 3H). Beyond 4h of release, the levels of pChk2, pChk1, yH2Ax, and p53 started to decrease in control cells, implying efficient DNA repair (Figure 3H). However, MANCR-depleted cells continued to show increased levels of checkpoint proteins beyond 4h of release (see 4h, 6h and 8h release) (Figure 3H). The defects in cell cycle progression observed in MANCR-depleted cells post-DNA damage could be due to an inefficient DNA damage response (DDR). Our results indicate that under normal circumstances, MANCR negatively regulates cell proliferation. However, upon DNA damage, MANCR levels are induced for efficient DDR.

An earlier study reported that MANCR-depletion resulted in defective mitosis, especially during cytokinesis.²⁰ PI-flow cytometry analyses in control and MANCR-depleted cells did not show significant change in the overall mitotic population (data not shown). Therefore, cells were stained with DAPI, and we calculated the percentage of mitotic cells in control and MANCR-depleted M4 cells. We observed a notable decrease in the percentage of mitotic cells when MANCR transcription was inhibited by CRISPRi approach, but not in the cells where MANCR RNA was depleted using shRNA (Supplementary Figure 3Ga). However, we did not see any significant differences in the percentage of specific substages of the mitotic cell population upon MANCR depletion (Supplementary Figure 3Gb).

MANCR promotes BrCa cell metastasis

Since MANCR is overexpressed in metastatic BrCa cells, we determined whether MANCR plays any role in tumor invasion and metastasis. MANCR-depleted M4 cells showed a significant decrease in in vitro cell migration (Figure 4Aa and b) and invasion (Figure 4Ba and b) as observed by Boydon chamber migration and Matrigel invasion assays respectively. Live cell wound healing assay also revealed that MANCR-depleted MDA-MB-231 cells had reduced wound-healing

ability over control cells (Figure 4Ca and b). Powered by actin polymerization, lamellipodia on the epithelial cell membrane play vital roles in promoting cell migration and invasion.³³ Significantly, MANCR-depleted cells showed less prominent lamellipodia (Figure 4D: see arrow). MANCRdepleted cells also showed prominent actin stress fibers compared to control cells (Figure 4D). Earlier studies reported that actin stress fibers mitigate cell motility. 34,35 Lack of lamellipodia and increased actin stress fibers in MANCR-depleted cells could be exerting a substantial influence on reduced migration and invasion. Finally, we tested the role of MANCR in cancer cell colonization of lung metastatic site in a murine model. Control and MANCR-depleted M4 cells were tail-vein injected in nu/nu athymic mice, and their colonization in the lungs was assessed. Control M4 cells showed prominent tumor nodules within the lungs, which were assessed visually upon necropsy (Figure 4Ea). MANCR-depleted cells result in decreased lung metastatic burden as determined by scoring visible tumors at necropsy. These observations were confirmed by histology (representative micrographs shown in Figure 4Eb). The results from in vitro and in vivo experiments indicate a potentially pivotal role for MANCR IncRNA in promoting cancer cell invasiveness, migration, and metastasis.

MANCR regulates the expression of genes maintaining genome stability

MANCR is a chromatin-enriched IncRNA. Chromatin RNAs regulate gene expression in cis or trans by modulating transcription and RNA processing.^{5,36,37} Consequently, we sought to investigate whether MANCR regulated the expression of genes, controlling cell cycle and genome stability. Using RNA-seq of control and MANCR-depleted (shRNA and CRISPRi) M4 cells, we observed differential expression of several thousand genes upon MANCR depletion (Figure 5A and Supplementary Table 2). For example, MANCR knockdown cells, achieved through shRNA, exhibited the upregulation of 2223 genes and the downregulation of 1626 genes (> 2-fold or more) (Supplementary Table 2). Cells depleted of MANCR using the CRISPRi approach displayed similar trends, showing upregulation and downregulation of 2569 and 1911 genes, respectively (Supplementary Table 2). We focused our efforts on the common subset of genes (2709 genes) that showed concordant expression changes in both MANCR sh and CRISPRi-treated cells. GO analyses revealed that they play crucial roles in several molecular processes (Figure 5B). The major node consisted of processes associated with DNA double-strand break repair, DNA replication, and cell cycle. The other node consisted of processes controlling mitosis, such as sister chromatid segregation, mitotic nuclear division, and kinetochore organization. The altered expression of DNA repair and cell cycle genes upon MANCR depletion may explain the aberrant cell cycle phenotype that we observed in MANCR-depleted cells.

To understand the interplay of MANCR and the patterns observed following its disruption, we explored the global distribution of the common set of genes sensitive to MANCR sh

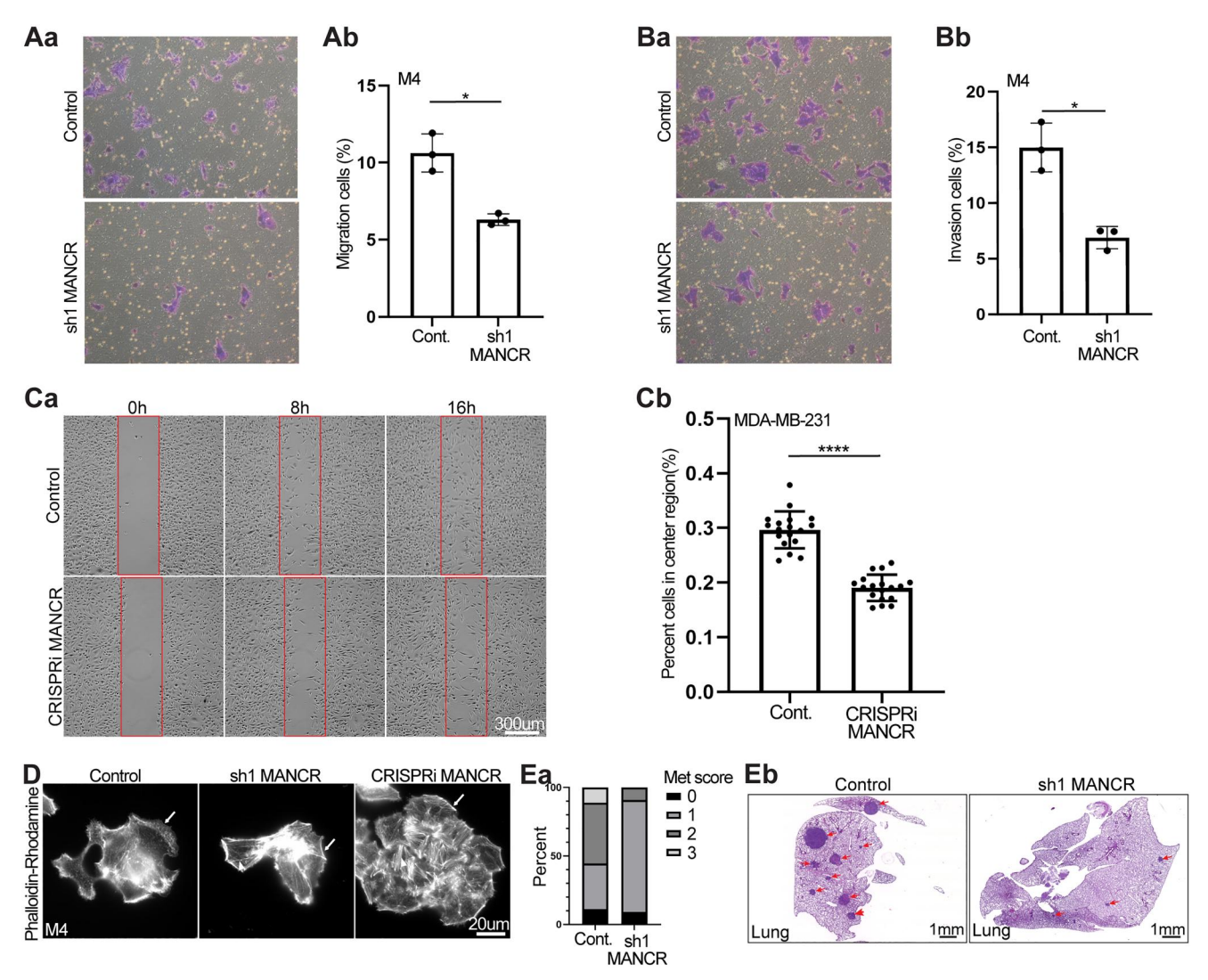


Figure 4. MANCR promotes metastasis. (A) The representative migration image (Aa) and quantification (Ab) of M4 WT and MANCR-depleted M4 cells. (B) The representative invasion image (Ba) and quantification (Bb) of M4 WT and MANCR-depleted M4 cells. (C) The wound healing assay (Ca) and quantification (Cb) of MDA-MB-231 WT and MANCR-depleted cells. (D) Phalloidin-rhodamine staining of actin filament in M4 WT, MANCR-depleted (shRNA1 and CRISPRi) cells. Scale bar = 20 μm. Arrow designates lamellipodia in WT cells. (E) Resulting lung metastatic burden in animals injected with M4WT and MANCR-depleted M4 cells. (Ea) Macrometastases that were visible were assessed at necropsy and scored based on number of visible metastases as follows: Score of 0 for no nodules, 1 for 1-3 nodules, 2 for 4-6 nodules and 3 for 7-9 nodules. (Eb) Representative micrographs of lungs of mice grafted with control or MANCR-depleted M4 cells. Arrows show metastatic nodules. Scale bar = 1 mm. Data were presented as mean \pm SD. Statistical analysis was conducted using unpaired two-tailed t tests. Significance levels were denoted as follows: *P < 0.05, **P < 0.01, ***P < 0.001, ****P < 0.0001. The same statistical approach was applied consistently across all panels if not specified.

and CRISPRi-treated cells. Many chromatin IncRNAs regulate the expression of proximal genes in cis and usually exert cis-regulatory function by associating with the regulatory element of the gene.^{5,36,37} In general, IncRNAs and their cisregulated genes exhibit a highly correlated expression pattern compared to unrelated genes.³⁸ Therefore, we considered whether MANCR-proximal genes are uniquely sensitive to the disruption in BrCa cells when compared against a genome-wide survey of local gene dynamics following MANCR silencing. Here, local sensitivity scores were determined by comparing our observed MANCR-disrupted gene expression patterns against a randomization-based null distribution. This comparison was made using a sliding window approach with a window size of 1 megabase (Mb) and a step size of 5 kilobases (Kb). MANCR-sensitive gene "hotspots" were thereafter defined as any 1 Mb window (centered on 5 kb bins) with dynamic local gene expression patterns having a distribution

false discovery rate (FDR) < 0.05 in MANCR-depleted cells (common gene sets identified by MANCR sh and CRISPRitreated cells). By this approach, we found that all MANCRsensitive gene hotspots reside in genomic intervals with patterns of concurrent downregulation across local genes (Figure 5Ca). Notably, of the three contiguous MANCR-sensitive gene hotspots predicted on chromosome 10, we found that the MANCR gene was located less than 400 Kb upstream from an annotated hotspot (Figure 5Cb). As a distribution, we noted that MANCR-sensitive hotspots tend to align with intervals characterized by high gene density. Hence, the likelihood of localization within or equidistant to a hotspot was not notably significant (P = 0.10 Figure 5Ca and b). Nevertheless, this observation is meaningful and establishes a putative link between MANCR and its proximal gene neighborhood, consistent with the possibility of cis regulation as described for other IncRNAs.

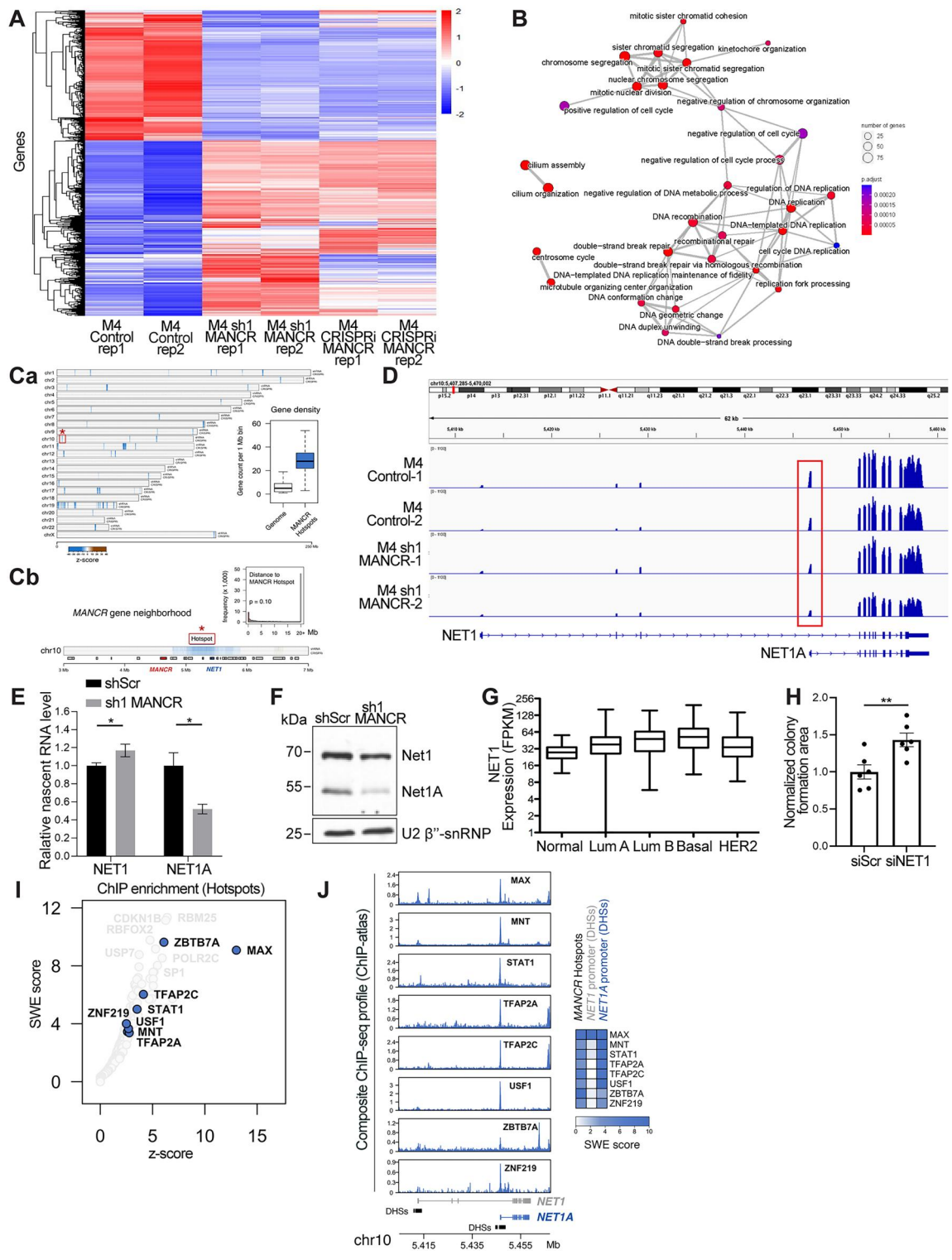


Figure 5. MANCR regulates cell cycle progression by modulating NET1A expression. (A) Heatmap showing differentially expressed genes in M4 WT, MANCR-depleted (shRNA1 and CRISPRi) M4 cells. (B) Biological process of commonly differentially expressed genes in MANCR-depleted M4 cells (MANCR CRISPRi and shRNA) compared to M4WT through GO. (C) Genome-wide (Ca) visualization of MANCR "hotspots"—defined as genomic windows with significant local MANCR sensitivity compared against a randomization-based null distribution (FDR < 0.05 in both MANCR shRNA1 and CRISPRi knockdown). Z-score represents the number of observed standard deviations from a permutation-derived expectation, tied to a given gene count. MANCR-proximal hotspot (Cb) shown with emphasis on MANCR and NET1/ NET1A genes. Histogram represents the probability of an annotated gene localizing within a specified genomic distance of a MANCR-sensitive hotspot (300 Kb bin size). (D) NET1/NET1A RNA peak enrichment in M4WT and MANCR-depleted cells using IGV browser. The red rectangle indicates an exon exclusive to NET1A. (E) RNA level of NET1 and NET1A in M4 scramble and MANCR shRNA1 knockdown cell lines measured by RT-qPCR. Data were presented as mean ± SD. Statistical analysis was conducted using unpaired two-tailed t tests. Significance levels were denoted as follows: *P < 0.05, **P < 0.01. The same statistical approach was applied consistently across all panels if not specified. (F) Protein level of NET1 and NET1A in M4 WT and MANCR shRNA1 knockdown cell lines measured by immunoblot. (G) Expression (fragments per kilobase million, FPKM) of NET1 (both NET1 and NET1A isoforms) in different subtypes of normal individual and breast cancer patients. (H) Long-term proliferation of M4 scramble and NET1 shRNA knockdown cells measured by colony formation assay. (I) ChIP enrichment survey for MANCRsensitive hotspots. Z-score represents the number of standard deviations observed for a given TF/chromatin factor from a randomization-based null model. SWE = significance weighted enrichment score (log2 (obs/exp) * -log10 (permutation p-val)). Features related to NET1A promoter are highlighted in blue. (J) Composite ChIP-seg signal and enrichment scores for candidate NET1A-related regulatory factors enriched broadly in MANCR-sensitive hotspots. Signal represents the upper quartile of all currently available, normalized signal values (ChIP-atlas). Complementary heatmap depicts significance-weight enrichment scores at MANCR-hotspots, NET1 promoter DHSs, (DNase-hypersensitive sites), and NET1A promoter DHSs.

Net1 (Neuroepithelial transforming gene 1) is a candidate gene of significant interest located in the MANCR-proximal hotspot on Chr 10 (Figure 5Cb, Supplementary Figure 4A). NET1 is a RhoA/RhoB-specific quanine nucleotide exchange factor (Rho-GEF) that regulates Rho-GTPase activity. 39,40 The NET1 gene codes for two functional isoforms (Net1 and NET1A), differ in their N-terminal regulatory domains, and are transcribed from two distinct promoters. 39,40 The longer NET1 isoform regulates mitotic progression, 41 whereas the shorter nuclear-localized NET1A isoform modulates cell motility, extracellular matrix invasion, tumor progression, and lung metastasis. 42-44 At the molecular level, NET1A isoform controls myosin-chain phosphorylation and regulates trailing edge retraction during cell migration.⁴³ NET1A isoform is also shown to be required for efficient DNA DSB repair, 45 and is overexpressed in BrCa. 42-44,46-49 Both MANCR and NET1A seem to function in similar cellular processes. Their depletion impacts cell proliferation, migration, and DNA damage response. Our RNA-seq data revealed that MANCR-depleted cells showed reduced levels of NET1A mRNA, but not the long NET1 isoform (Figure 5D). RT-qPCR also confirmed reduced levels of total NET1 in MANCR-depleted cells (Supplementary Figure 4B and C). Since NET1 and NET1A isoforms are transcribed from distinct promoters, we tested whether the differential expression of NET1A/Net1 observed in MANCR-depleted cells was due to differential transcription. Nascent RNA pull-down followed by RT-qPCR analyses affirmed that MANCR-depleted cells reduced the transcription preferentially from the NET1A promoter and not the NET1 promoter (Figure 5E). Furthermore, immunoblot assay revealed a significant reduction in the levels of the NET1A isoform (Figure 5F) in MANCR-depleted M4 cells. Like MANCR, NET1 gene was also preferentially overexpressed in basallike/TNBC patients, as observed by gene expression analyses using TCGA BrCa patient data (Figure 5G). Likewise, M4 cells tend to have higher levels of NET1 over M1 cells (Supplementary Figure 4D). Finally, NET1- or MANCR-depleted M4 cells showed similar cell cycle defects, including increased cell proliferation and defects in cell cycle progression post-HU-mediated DNA damage (Figure 5H and Supplementary Figure 4Ea and b). Based on these results, we hypothesize that in TNBC cells, MANCR regulates DDR and possibly cellular metastasis by modulating differential expression of the NET1A isoform in cis.

Differential binding of TFs and/or chromatin-associated factors could influence the isoform-specific expression of NET1/NET1A that we observed in MANCR-depleted cells. More broadly, we hypothesize that specific downregulation of NET1A in MANCR-depleted cells is likely an example of a larger network of dynamic transcription patterns driven by the intersection of MANCR disruption and differential TF activity. Therefore, we revisited MANCR-sensitive hotspots to identify candidate regulatory factors enriched within these genomic intervals, integrating > 10,000 ChIP-seq experiments uniformly processed and resourced through ChIP-atlas.⁵⁰ Using this approach, we found that MAX, a bHLHZ transcription factor that drives dynamic gene activity through interactions with coregulatory factors, was among the most significantly enriched features within MANCR-sensitive

hotspots (Figure 51). MAX was also prominently enriched at the NET1 gene, with stronger occupancy patterns observed at the NET1A promoter compared to NET1 (Figure 5J). Further investigation of enriched features within MANCR-hotspots and NET1A uncovers a multitude of factors that were notably enriched at NET1A compared to NET1 promoter, including MAX-interacting protein, MNT, transcription factor AP-2 alpha and gamma (TFAP2A/2C), and zinc finger proteins ZNF219 and ZBTB7A (Figure 5I and J). These data point to putative mechanistic underpinnings of dynamic expression following MANCR disruption, and altogether suggest that multiple regulatory networks converge on NET1A and other MANCR-sensitive genes.

MANCR modulates RNA processing

The majority of IncRNA regulates gene expression by interacting with protein(s), influencing their localization and activity. 5,36,37 Here, we looked for any potential interacting protein partner/s of MANCR using an RNA pull-down assay. We performed RNA pull-down in M4 (control and HU-treated samples in biological quadruplicates) nuclear extract with biotin labelled full-length MANCR or eYFP (as negative control) RNA followed by mass spectrometry. Mass spectrometry analysis revealed numerous proteins as potential interactors of MANCR (Supplementary Table 3). Several histone protein isoforms preferentially associated with MANCR only in HUtreated cells. Strikingly, MANCR interacted with γH2AX, the marker of double-strand DNA damage sites, in control and not in the DNA damaged cell extracts (Supplementary Table 3). The interaction between MANCR and histone proteins could be due to MANCR's association to chromatin. Prominently, MANCR interacted with two RNA binding proteins (RBPs), hnRNP L (heterogenous nuclear ribonucleoprotein) and LUC7L, in both control and DNA damage cell extracts (Supplementary Table 3). With an in vitro biotin-RNA pull-down followed by immunoblotting, we validated the interaction between MANCR and hnRNP L (Figure 6A) but not with LUCL7 (data not shown). The endogenous hnRNP L and MANCR interaction was confirmed by RNA-immunoprecipitation (RNA-IP) followed by RT-qPCR analysis (Figure 6B).

hnRNP L is an RNA processing factor that regulates alternative mRNA splicing by binding to exon splicing silencer elements.^{51,52} It also functions in the mRNA export of intronless genes and mRNA stability. hnRNP L preferentially recognizes CA repeats within the RNA.53,54 MANCR IncRNA contains three distinct regions with CA repeats (Figure 6C). An in vitro RNA pull-down followed by immunoblotting assays using cloned fragments of MANCR containing each of these three CA repeat regions (509 bp, 466 bp and 508 bp) revealed that hnRNP L bound to multiple regions within the MANCR RNA (Figure 6D). These results signify that MANCR may interact with multiple copies of hnRNP L. LncRNAs titrate the levels of hnRNPs and chromatin-interacting proteins, thereby regulating the association of these proteins to specific substrate genes/RNAs.^{5,36,37} We investigated whether MANCR modulates the association between hnRNP L and NET1A RNA. hnRNP L RIP-RT-qPCR revealed that MANCR-

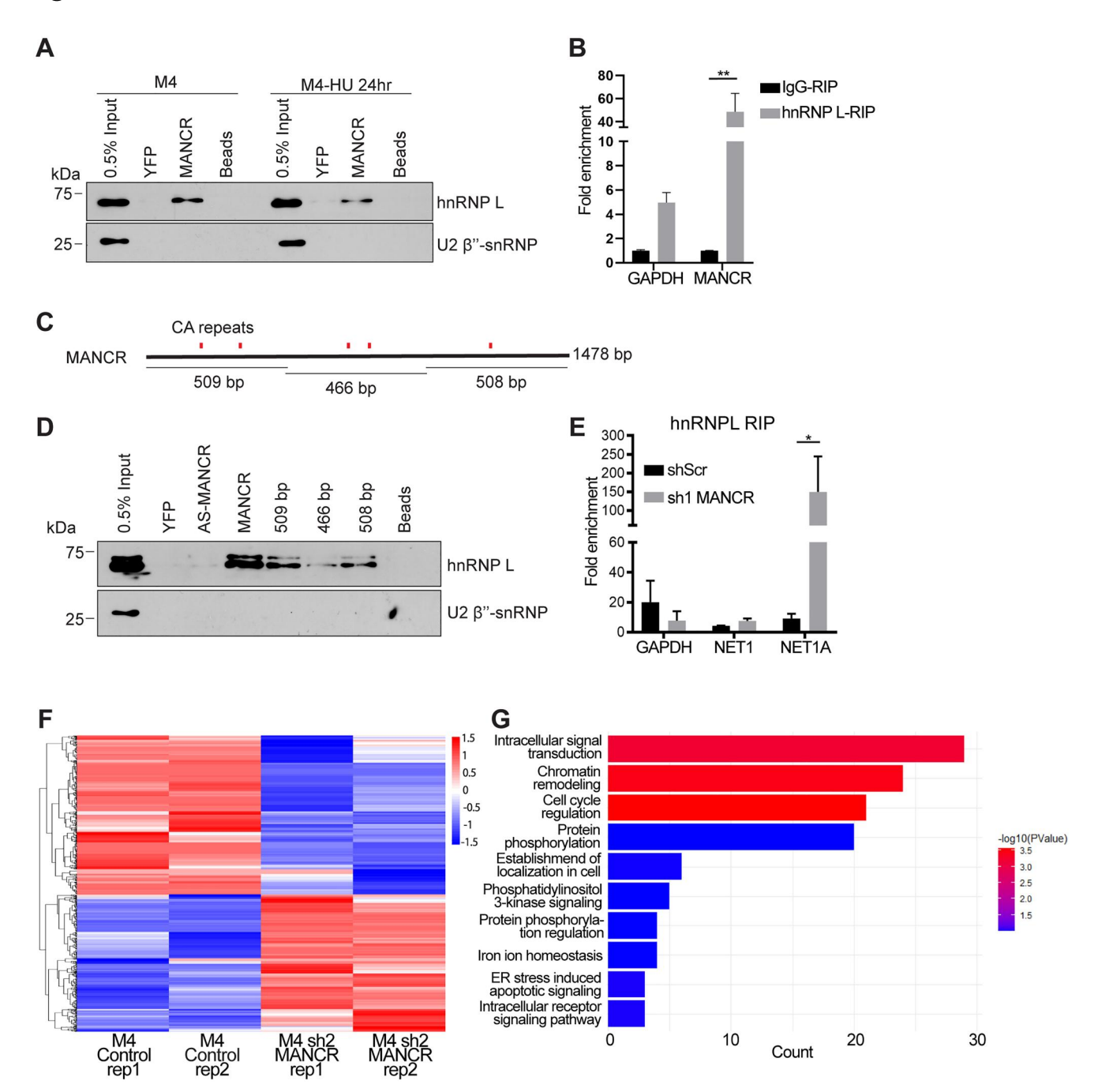


Figure 6. MANCR interacts with hnRNP L and influences pre-mRNA processing. (A) Biotinylated MANCR RNA pull-down in M4 nuclear extract (control and HUtreated) followed by immunoblotting with hnRNP L antibody. U2B" snRNP was used as a negative control. (B) MANCR-hnRNP L interaction measured by hnRNP L RNA immunoprecipitation followed by RT-qPCR. IgG was used for normalization, and GAPDH was used as a negative control. (C) CA repeats distribution in MANCR transcript. (D) Biotinylated MANCR (full length, antisense and different MANCR fragments) RNA pull-down in M4 cell extract followed by immunoblotting with hnRNP L antibody. YFP and MANCR antisense were used as negative controls for pull-down. U2B" snRNP was used as negative control for immunoblotting. (E) HnRNP L binding on NET1 and NET1A mRNA analyzed by hnRNP L RNA-IP followed by RT-qPCR. IgG was used for normalization. (F) Heatmap of differentially spliced exons in control and MANCR shRNA2-depleted M4 cells. Heatmap color indicates relative inclusion level of differential spliced exons, wherein red indicates more inclusion and blue indicates less inclusion. (G) Biological process of differentially spliced genes in MANCR shRNA2 knockdown cells compare to M4 WT through gene ontology (GO). Data were presented as mean ± SD. Statistical analysis was conducted using unpaired two-tailed t tests. Significance levels were denoted as follows: *P < 0.05, **P < 0.05. The same statistical approach was applied consistently across all panels if not specified.

depleted cells exhibited a significantly enhanced interaction between hnRNP L and NET1A RNA, while no such effect was observed with NET1 transcripts (Figure 6E). This result implies that by binding to multiple copies of hnRNP L MANCR quenches the interaction between hnRNP L and other RNAs in *cis.* Finally, we established whether MANCR influences NET1 mRNA levels/stability by modulating hnRNP L interaction. We determined NET1/NET1A RNA levels in control

and hnRNP L-depleted M4 cells (Supplementary Figure 5A). Saliently, M4 cells, stably depleted of hnRNP L, showed reduced levels of MANCR (Supplementary Figure 5B). We observed a small but nonsignificant change in the levels of NET1 RNA isoforms upon hnRNP L depletion. These results suggest that hnRNP L regulates MANCR expression. Based on our data, we proposed that MANCR sponges hnRNP L by binding to it through the CA-rich repeat regions and



inhibiting hnRNP L binding to NET1A transcript under normal conditions. In the absence of MANCR, the free hnRNP L binds NET1A transcripts and potentially triggers degradation.

Since MANCR interacts with hnRNP L, we determined whether MANCR regulates RNA processing by modulating the RBP activities. We performed a deep poly A + RNA-seg in control and MANCR KD M4 cells and assessed that MANCR depletion impacts mRNA processing. MANCR-depleted cells showed altered mRNA splicing of ~1000 events (0.05 FDR; 15% or more PSI) (Figure 6F and Supplementary Table 4) compared to control cells. This included 659 skipped exons, 106 retained introns, 51 mutually exclusive exons, 86 alternative 5' splice sites, and 59 alternative 3' splice site events (Supplementary Table 4). GO analyses revealed that MANCRregulated alternative splicing of genes by controlling key processes such as signal transduction and cell cycle regulation (Figure 6G).

Discussion

Triple negative breast cancer (TNBC) is the most aggressive form of BrCa molecular sub-type and often entails a poor prognosis and low survival rate. Aberrant expression of IncRNAs, which play vital roles in regulating gene expression, contribute to various cancers, including BrCa. Studies from our laboratory and other laboratories have demonstrated the role of IncRNAs in BrCa progression. 6,8,10,11,55-58 In the present study, we delve into the roles of MANCR, one of the least understood and unexplored TNBC-specific IncRNAs, shedding light on its significance in BrCa progression and metastasis.

Induced in response to DNA damage, MANCR regulates the DDR, as evidenced by defective DDR, accompanied with altered expression of genes, controlling DDR in MANCRdepleted TNBC cells. An earlier study also reported the potential involvement of MANCR in BrCa genome stability.²⁰ In general, TNBC tumors show high levels of genomic instability, primarily due to defective DDR pathways. 30,31 Like MANCR, proteins controlling DDR are often overexpressed in TNBC, but often their loss promotes genome instability, leading to cancer progression. 31,59,60 For example, DDR proteins such as PARP1, BRCA1, and XRCC1, which are well-characterized as tumor suppressors and restrict uncontrolled cell proliferation, are often overexpressed in TNBC. 30,31,60 propose that in TNBC, MANCR is induced in response to inherent DNA damage for efficient DDR.

The present study indicates MANCR as a negative regulator of BrCa cell proliferation. However, an earlier study reported MANCR to promote BrCa cell proliferation.²⁰ In the previous study, the authors observed that MDA-MB-231 cells depleted of MANCR, using modified LNA ASOs (antisense oligonucleotides), showed reduced cell proliferation, viability, and increased DNA damage. Furthermore, the authors reported mitotic defects, including defective cytokinesis, upon MANCR depletion. Contrary to this, we observed that depletion of MANCR in three independent TNBC cells (M4, MDA-MB-231, and MDA-MB-468) resulted in increased cell

proliferation, as evaluated by short-term and long-term cell proliferation assays. In addition, overexpression of MANCR in a nontumorigenic, endogenous MANCR nonexpressing MCF10A (M1) cells resulted in reduced cell proliferation, further supporting the negative role of MANCR in cell proliferation. Moreover, we did not observe cytokinesis defects in MANCR-depleted cells. The primary difference between the two studies is that we assessed the phenotypes in three TNBC cell lines after stably knocking down MANCR RNA (shRNAs) or MANCR transcription (CRISPRi). In contrast, the earlier study utilized transient depletion of MANCR using LNA-based ASOs. It is not clear whether short-term versus long-term depletion of MANCR may result in different cell phenotypes.

We observed that MANCR promoted the expression of NET1A isoform, a nuclear Rho-GEF, known to regulate cell survival post-DSBs. 61,62 In BrCa cells, NET1A was induced during DNA damage, and its depletion protected cells from DNA damage-induced cell death.⁶² NET1A-depleted BrCa cells fail to repair DSB post-DNA damage. 45 NET1A isoform also regulated ATM activity following DSB and was required for efficient DNA repair and cell survival.45 MANCR-depleted cells showed reduced levels of NET1A mRNA and protein. In addition, both MANCR or NET1 depleted TNBC cells showed similar cell proliferation defects, implying that both may regulate similar cellular processes. We speculate that MANCR modulates cell survival by influencing the transcription of NET1A in cis. LncRNAs are known to regulate transcription of genes in cis by influencing the recruitment or association of chromatin or transcription factors (TFs). 5,36,37,63-66 Conversely, transcription from the IncRNA gene locus reshapes the local chromatin structure, thereby influencing the expression of genes located in genomic proximity. 5,36,37,63-66 We discerned a distinct preference in MANCR for selectively enhancing the transcription of NET1A over NET1. This observation hints at the potential influence of MANCR on orchestrating specific interactions among TF/co-factors and chromatin regulatory proteins within the NET1/NET1A promoters. Previous studies demonstrated differential association of specific TFs/co-factors between NET1 and NET1A promoters. 67,68 For example, short-term TGF-β treatment selectively induced only NET1A isoform via SMAD and MAPK/ERK signaling.⁶⁷ However, estradiol treatment, which activates ERα-mediated gene activation, preferentially induced the expression of NET1 and not NET1A in BrCa cells.⁶⁸ Our analyses indicate that several TFs implicated in cell cycle and cancer progression, such as MAX and TFAP2A/2C showed preferential binding to the NET1A promoter. In addition, these TFs showed high binding affinity to a significant number of MANCR-sensitive gene hotspots. It is possible that MANCR influences the association of these TFs to specific regulatory elements, such as that of NET1A, thus regulating expression. Future studies will determine how or whether MANCR modulates the association of TFs to the target genes.

The present and earlier studies indicate that MANCR promotes cancer metastasis.^{23,25} For example, we demonstrated that MANCR-depleted TNBC cells showed reduced cell migration, invasion, wound-healing response, lack of prominent lamellipodia, and increased presence of stress fibers. MANCR-

depleted cells also exhibited reduced metastatic colonization in the lung. The prometastatic function of MANCR may, in part, be explained by its role in selectively promoting NET1A expression. NET1 modulates the activity of the RhoA/RhoB sub-family of GTPases, which, by regulating cytoskeletal organization, play an essential role in cell polarity, adhesion, and migration.⁶⁹ NET1 is overexpressed in several cancer types, and high NET1 signaling correlates with increased incidence of metastasis, preferentially in TNBC/basal-like subtype. 42-44,46-49 A significant body of literature outlines a direct involvement of the NET1A isoform in promoting EMT, BrCa cell motility, migration, invasion, and metastasis. $^{42-44,46-49}$ For example, TGF- β -mediated activation of NET1A promotes EMT and cancer cell invasiveness. 67,70 Coexpression of NET1 along with $\alpha6\beta4$ integrin is recognized as a biomarker for identifying distant metastasis in BrCa patients.⁷¹ NET1 (long isoform) and NET1A (short isoform) execute independent roles in controlling specific cancer cell properties. NET1 isoform plays a role in promoting BrCa cell proliferation, whereas the NET1A isoform controls cell motility and migration. 20,68 For example, NET1A- and not NET1-depleted TNBC cells showed reduced trailing edge retraction and defects in Matrigel invasion.⁴³ In addition, NET1A preferentially regulates cell adhesion, TGF-β-stimulated actin cytoskeletal organization, and focal adhesion maturation.^{67,68,70,72} Loss of NET1 also reduced the number of metastatic nodules on lung,⁴⁴ a phenotype that we observed in MANCR-depleted cells. All these results support the hypothesis that MANCR promotes cancer cell metastasis by modulating the expression of NET1A in TNBC.

Our results indicated that MANCR inhibits cancer cell proliferation. But at the same time, it promotes cancer cell metastasis, implying two independent, and somewhat opposite roles for MANCR in cancer cell proliferation and metastasis. TGF- β is known to play pleotropic roles as a tumor suppressor and a prometastatic regulator.⁷³ In several cancer conditions, TGF-β inhibits cell proliferation, and key oncogenic signals inactivate TGF-β-Smad pathways to favor cancer growth. At the same time, tumors overproducing TGF-β, promotes tumor invasiveness, by accelerating several prometastatic processes, including epithelialmesenchymal transition. Tumor cell-secreted TGF-β also promotes cell metastasis by influencing the tumor microenvironment (TME). Another example includes, the Δ Np63, the isoform of TP63 gene, in which the oscillatory expression of Δ Np63 in BrCa tumor cells dictates tumor progression and metastasis in BrCa. The Δ Np63 levels are elevated in primary BrCa tumors and plays essential oncogenic role in the establishment of primary tumors, and during the later stages of metastasis, including extravasation and colonization. However, it was found that low levels of Δ Np63 promotes intravasation of primary tumor cells into the blood stream. These examples imply that genes, such as MANCR might play dual roles in tumor progression and metastasis by influencing independent cancer signaling events.

Materials and Methods

Cell culture and treatment

M1-M4 cell lines were cultured as described previously.⁷⁵ Briefly, M1 cells were prepared in an assay medium containing growth factor (DMEM/F12 with 5% horse serum, 1 mg/mL hydrocortisone, 1 mg/mL cholera toxins, 10 mg/mL insulin, 10 mg/mL EGF, and 1% penicillin/streptomycin along with 2% growth-factor reduced Matrigel). M3 and M4 cells were prepared in a similar medium but without EGF. MDA-MB-231 cells are obtained from ATCC and cultured in RPMI supplemented with 10% fetal bovine serum (FBS) and 1% penicillin/streptomycin. MDA-MB-468 cells are obtained from ATCC and cultured in DMEM supplemented with 10% fetal bovine serum (FBS) and 1% penicillin/streptomycin.

RNA-seq of M1-M4 cells and bioinformatics analysis

RNA was extracted using TRIzol reagent (Invitrogen) as per manufacturer's instructions. Samples for RNA-seq were further cleaned up by RNeasy Mini Kit (QIAGEN). The RNA-seq libraries were prepared with Illumina's TruSeq Stranded mRNAseq Sample Prep kit (Illumina). Paired-end, polyA + RNA-sequencing was performed on Illumina platform (Novaseg 6000) at the Roy J. Carver Biotechnology Center at UIUC. The RNA-seq data are deposited in GEO with accession number GSE257538. RNA-seq read quality was confirmed by FASTQC. RNA-seq reads were aligned to human reference genome GRCh38 assembly using HISAT2. For statistical analyses, raw gene counts were first analyzed by HTSEQ-Count, and then analyzed using edgeR. Categorization of gene type was extracted from GRCh38 assembly GTF file downloaded from Ensembl (v94, from https://useast.ensembl.org/info/data/ftp/ index.html). Hierarchical clustering of genes (rows) was performed with complete-linkage method. Differential expression analyses were performed using exactTest. Differentially expressed genes (DEGs) were defined by |fold change| > = 1.5-fold and FDR < 0.05. Gene ontology analyses (biological processes, KEGG pathway analyses) and GSEA (gene set enrichment analysis) were performed using clusterprofiler of Bioconductor.

Generation of stable cell lines

Lentiviral plasmids psPAX2 (Addgene #12260) and PMD2.G (Addgene #12259) were used for lentivirus production. In brief, psPAX2, PMD2.G and cargo plasmid were transfected into HEK293T cells at 1:1:1 ratio through Lipofectamine 3000 (Invitrogen) as per manufacturer's instructions. Then the lentivirus enriched supernatant was collected for reverse infection (https://www.addgene.org/protocols/generating-stable-celllines/) of target cell lines. The infected cell lines then underwent drug selection and gPCR confirmation for success infection. For shRNA knockdown, the lentiviral plasmid pLKO.1 puro (Addgene #8453) was inserted with shRNA sequence, then the infected cell line was selected by puromycin (Sigma, #P8833) at 2 µg/mL; for rescue/overexpression, full length MANCR was first cloned into pGEM-T (Promega) vector, then the MANCR fragments containing point mutations at shRNA recognition site are amplified through QuikChange II (Agilent Technologies). The fragments are inserted into lentiviral vector pCW57-MCS1-P2A-MCS2 (Hygro) (Addgene #80922), and the infected cell line was selected by



hygromycin (Sigma, #H7772) at 100 μg/mL. The MANCR rescue/overexpression is achieved by adding 1µg/mL doxycycline (Sigma, #D9891) and confirmed by qPCR (data not shown); for CRISPRi knockdown, the lentiviral dcas9-Krab (ZIM3) was first used for first round of infection for the target cell line, then the lentiviral lentiGuide-Puro (Addgene #52963) expressing MANCR gRNA (BsmBl site was used for fragment insertion) was used for second round of infection. The infected cell line was first selected by blasticidine (Sigma, #15205) at 12 µg/mL and then selected by puromycin (Sigma, #P8833) at 2 μg/mL. The drug concentration was reduced to half compared to the selection concentration after 7-day selection for maintenance.

Proliferation assay and colony formation assay

For proliferation assay, 1×10^5 cells were seeded per well in a 6-well plate, and the cell number will be counted by hemocytometer for every 24h; For colony formation assay, 1000 cells were seeded in a 6-well plate. After 2 to 3 weeks, colonies were washed with PBS twice, fixed with ice-cold methanol for 5 min and stained with staining solution (0.05% crystal violet dissolved in 10% methanol). Then the pictures of the plates were taken and analyzed by ImageJ add-on ColonyArea. The surface area covered by colony was measured for each well, and the ratio of experimental well to wild-type well was calculated as normalized colony formation area.

RNA extraction and quantitative real-time PCR (RTqPCR)

RNA was extracted using either TRIzol or TRIzol LS (Invitrogen) reagent as per the manufacturer's instructions. The concentration was measured using a Nanodrop instrument (ThermoFisher SCIENTIFIC). RNA was treated with RNase-free DNase I (Sigma) and reverse transcribed into cDNA by Multiscribe Reverse Transcriptase and Random Hexamers (Applied Biosystems). QPCR was carried out by StepOnePlus (Applied Biosystems).

Nuclear and cytoplasmic fractionation

M4 cells were scraped from the 10-cm plate and resuspended with solution A (10 mM HEPES pH7.9, 10 mM KCl, 1.5 mM MgCl2, 0.34 M sucrose, 1 mM DTT, 10% glycerol, RNase inhibitor and 0.1% Triton X-100) on ice for 5 min. The cytoplasmic fraction was collected from supernatant after centrifuging at 4° C at 1400 q for 4 min. The pellets (nuclei) were then washed with solution A without Triton X-100 twice, and then resuspended with solution B (3 mM EDTA, 0.2 mM EGTA and RNase inhibitor) and incubated on ice for 30 min. The nucleoplasm fraction was collected from supernatant after centrifuging at 4°C at 1700 g for 4 min. The chromatin fraction was collected from the pellets.

Single molecule fluorescence in situ hybridization (smFISH)

The smFISH was performed as described previously. 76 In brief, MANCR smFISH probe set was designed using Stellaris Probe Designer. Oligonucleotides with a 3' amino group were pooled and coupled with AF488 by incubation overnight at 37 °C in 0.1 M NaHCO₃. Cells were fixed with 4% PFA for 15 min at room temperature and permeabilized with 0.5% Triton X-100 for 10 min on ice. smFISH probes were added to Stellaris RNA FISH Hybridization Buffer with 10% formamide at a final concentration of 125 nM. Hybridization was carried out in a humidified chamber in the dark overnight at 37 °C. The coverslips were then washed with Stellaris RNA FISH Wash Buffer A and mounted in VectaShield Antifade Mounting Medium (Vector Laboratories). SmFISH images were taken using Axioimager.Z1 microscope (Zeiss) equipped with 63×/1.4 NA oil immersion objective and Zeiss Axiocam 506 mono camera with a z-interval of 0.24 mm or DeltaVision microscope (GE Healthcare) equipped with 60×/1.42 NA oil immersion objective (Olympus) and CoolSNAP-HQ2 camera.

Flow cytometry analysis

PI analyses: PI analyses were performed as per earlier study.⁷⁷ For flow cytometry, cells were collected and washed in cold PBS, resuspended in PBS + 1% NGS, and fixed in chilled ethanol overnight. Cells were then washed and resuspended in PBS + 1% NGS with 120 μ g/mL propidium iodide (PI) and $10 \,\mu g/mL$ RNase A for 30 min at 37 °C. DNA content was measured by flow cytometry. For analysis, we gated the single cell population using width vs area. This gate was then applied to the scatter plot and the debris was ungated. Finally, the gates were applied to the PI histogram plot. Specifically, data were gated on single cells from 2C to 4C DNA content.

BrdU-PI analyses: M4 cells were incubated in culture medium containing 50 μM BrdU for 1 h prior to collection. Cell pellets were washed once with 1% BSA in PBS, centrifuged at 4°C, 3500 rpm for 15 min, resuspended with 0.9% NaCl solution and then fixed by dripping another one volume of prechilled absolute ethanol. After overnight fixation at −20 °C, samples were centrifuged at 4°C, 3500 rpm for 15 min to remove supernatant. Cell pellets were then treated with 2N HCl containing 0.5% Triton-X 100 for 25 min on rotator at room temperature to denature DNA, followed by neutralization with 0.1 M Na₂B₄O₇ solution. Each cell sample was then labeled with 10 μL BD Pharmingen[™] FITC mouse-anti-BrdU (BD #556028) diluted in 50 µL 1% BSA/0.5% Tween-20 in PBS at room temperature for 1 h. After washing once with PBS, cells were incubated in PBS $+ 24 \mu g/mL$ propidium iodide (PI) + $10\,\mu g/mL$ RNase A at $37\,^{\circ}C$ for 1 h. Samples were filtered through cell strainer and analyzed with BD® LSR II Flow Cytometer. Data processing was completed in FCS Express 5.

Migration and invasion assay

Cells were grown in regular media until 50% confluency then the medium was changed to low serum medium (1% HS in DMEM/F12) for 12 h. Cells were harvested using trypsin and

resuspended in low serum medium to a concentration of 2000 cells per microliter for the migration assay (Corning 354578) and 5000 cells per microliter for the invasion assay (Corning 354483). 100 µL of the cell suspension was added to the upper chamber of the transwell and the lower chamber of the transwell was filled with 700 µL of the regular growth media. The transwell plate was then put in the incubator for 24 h. The nonmigrated/-invaded cells in the upper chamber of the transwell were scraped off thoroughly before fixing the cells and staining with 0.05% crystal violet in 10% methanol.

For the invasion assay, the matrigel-coated transwells were thawed to room temperature then incubated with low serum media at 37 °C to rehydrate before seeding the cells.

Wound healing assay

Cells were grown in regular media until confluency then the medium was changed to low serum medium (1% HS in DMEM/F12) for 12 h. Scratches were drawn using a sterile 10 μL pipette tip and the cells were rinsed twice with low serum medium to remove the debris and floating cells. Cells were allowed to migrate at 37 °C and the wound area was imaged every 15 min. Total migrated cells was calculated using the 0 and 16 h time points for each position. Five positions were chosen per replicate and the experiment was performed in triplicate.

Xenograft studies

All procedures involving animals had been previously approved by the University of Illinois IACUC. Xenografts were carried out similarly to previously described.⁷⁸ For primary tumors, cells were grafted orthotopically into the axial mammary fat pad of female nu/nu mice. Subsequent tumors were monitored by direct caliper measurement. For lung colonization experiments, cells were grafted intravenously into female nu/nu mice. After 50 days, mice were euthanized, and lungs were formalin-fixed for histologic analysis.

Net1A gene expression in TCGA

Net1 expression was analyzed using the BRCA TCGA RNA-seq (https://xenabrowser.net/datapages/?dataset=TCGA. BRCA.sampleMap/HiSeqV2&host=https://tcga.xenahubs.net). For each tumor, the subtype was matched from published data.⁷⁹

MANCR-sensitive hotspot analysis

To define local windows with significant gene sensitivity following MANCR disruption, a randomization-based statistical approach was applied using a sliding genomic window of 1 Mb with 5 Kb step-size (resolution). Differential gene expression (DGE) statistics were transformed to significanceweighted fold change (SWFC) for both MANCR shRNA1 and CRISPRi experiments. The SWFC statistic for each gene was then tied to a single genomic coordinate corresponding to a

given gene's transcription start site, averaged across all annotated start sites wherever applicable. For each 5 Kb bin, the median SWFC statistic for the distribution of genes within 1 Mb (500 kb upstream, 500 Kb downstream) were compared against an empirical null distribution, tied to the observed number of genes (n) in each window. For each window, an expected median SWFC was derived by random sampling of (n) number of genes from the DGE distribution, with each interval then assigned a permutation P value and z-score (number of standard deviations from the permutation mean). Permutation P values were subsequently adjusted using the Benjamini-Hochberg method (false discovery rate), and MANCR-sensitive hotspots defined as any genomic window with an FDR < 0.05 in both MANCR shRNA1 and CRISPRi experiments.

ChIP-seq enrichment analysis and visualization

Transcription factor (TF) overlap with MANCR hotspots, NET1 promoter DNase hypersensitive sites (DHSs), and NET1A DHSs were determined using the ChIP-atlas resource of uniformly processed ChIP-seq datasets.⁵⁰ DNase I hypersensitive sites were retrieved from https://www.encodeproject.org/files/ ENCFF503GCK/ and restricted to elements within ±2 Kb of either NET1 or NET1A promoter. Individual TF enrichment scores were determined by comparing the observed overlap frequency of each respective TF for a given set of genomic intervals (i.e., hotspots or promoter DHSs) against a randomization-based null distribution, determined by permuting the same number of (random) ChIP-seq experiments. The enrichment of each feature was assessed by standardization (zscore) and significance-weighted enrichment. ChIP-seq pileup signal tracks for TFs of notable interest were visualized by computing the upper quartile signal value across all available ChIP-seg signal files, uniformly processed by ChIP-atlas.⁵⁰

Northern blot

Poly A + RNA was isolated from total RNA using the NucleoTrap mRNA Mini Kit (Macherey-Nagel). Next, 10 μg of Poly A + RNA from either M3, M4 or MA-MB231 cells were separated on a 1% agarose gel, which was prepared with Northern Max Denaturing Gel Buffer (Ambion) and run in Northern Max Running Buffer (Ambion). The RNA was then transferred to an Amersham Hybond-N + blot (GE Healthcare) via capillary transfer in 10X SSC and crosslinked to the blot by UV (254 nm, 120 mJ/cm²). The DNA probes specific to MANCR were labeled with $[\alpha - 32P]$ dCTP by the Prime-It II Random Primer Labeling Kit (Stratagene), as per the manufacturer's instructions. Hybridization was carried out overnight at 42 °C using ULTRAhyb Hybridization Buffer (Ambion) containing 1×10^6 cpm/mL of denatured radiolabeled probes. Finally, the blots were washed with $2\times$ SSC, 0.1% SDS, $1\times$ SSC, 0.1% SDS, and 0.1 \times SSC, 0.1% SDS and developed using a phosphor-imager.



RNA stability assay

RNA stability assay from M4 cells was performed by treating cells with actinomycin D (2 µg/mL) followed by isolating RNA using TRIzol reagent. RNA levels were estimated by qRT-PCR at different time points post Act-D treatment, and half-life was estimated by analyzing Ct values.

Nascent RNA capture assay

Nascent RNAs were labeled and captured using a Click-iT Nascent RNA capture kit (Invitrogen #C10365) per the manufacturer's instructions. Expression levels of nascent RNAs were quantified by qRT-PCR.

RNA pull-down followed by mass spectrometry analyses

MANCR and the control YFP or AS-MANCR cDNA were used to perform in vitro transcription to generate biotinylated MANCR and the control RNAs using MEGAscript in vitro transcription kit (Ambion) and biotin RNA labeling mix (Roche). The in vitro transcribed RNA was treated with DNase (Ambion) and purified with RNeasy kit (Qiagen). The nuclear lysate was precleared by incubation with Dynabeads M-280 Streptavidin (Thermo Fisher Scientific) for 4h at 4°C. One microgram of biotinylated RNA was incubated with 2 mg precleared nuclear lysate prepared from M4 control or HU treated cells for 3 h at 4 °C. The biotinylated RNA-protein complexes were pulled down by incubation with Dynabeads M-280 Streptavidin (Thermo Fisher Scientific) for 4h at 4°C. RNA-protein complex bound to the beads were washed with high salt buffer, low salt buffer and TE buffer for 10 min each, and finally eluted with SDS-PAGE sample buffer by boiling at 95 °C for 5 min. Interacting proteins were fractionated by SDS-PAGE and each lane cut into 10 slices. The protein bands were then in-gel digested with trypsin (Thermo) overnight at 37 °C, as described.80 The peptides were extracted following cleavage and lyophilized. The dried peptides were solubilized in 2% acetonitrile, 0.5% acetic acid, 97.5% water for mass spectrometry analysis. They were trapped on a trapping column and separated on a 75 μm x 15 cm, 2 μm Acclaim PepMap reverse phase column (Thermo Scientific) using an UltiMate 3000 RSLCnano HPLC (Thermo Scientific). Peptides were separated at a flow rate of 300 nL/min followed by online analysis by tandem mass spectrometry using a Thermo Orbitrap Fusion mass spectrometer. Peptides were eluted into the mass spectrometer using a linear gradient from 96% mobile phase A (0.1% formic acid in water) to 55% mobile phase B (0.1% formic acid in acetonitrile) over 30 min. Parent full-scan mass spectra were collected in the Orbitrap mass analyzer set to acquire data at 120,000 FWHM resolution; ions were then isolated in the quadrupole mass filter, fragmented within the HCD cell (HCD normalized energy 32%, stepped \pm 3%), and the product ions analyzed in the ion trap. Proteome Discoverer 2.0 (Thermo) was used to search the data against human proteins from the UniProt database using SequestHT. The search was limited to tryptic peptides, with maximally two missed cleavages allowed. Cysteine carbamidomethylation was set as a

modification, and methionine oxidation set as a variable modification. The precursor mass tolerance was 10 ppm, and the fragment mass tolerance was 0.6 Da. The Percolator node was used to score and rank peptide matches using a 1% false discovery rate.

RNA immunoprecipitation (RIP)

M4, M4 control, and M4-shMANCR cells were cross-linked with 4% formaldehyde. The cross-linking was stopped by 0.125 M Glycine, and cells were washed with 5 mL PBS. Cells were lysed with buffer B (1%SDS, 10 mM EDTA, 50 mM Tris-Cl pH 8.1, protease inhibitor cocktail, and RNase inhibitor). The whole cell lysate was sonicated at high settings for 15 min to prepare a fragment size ranging between 200 and 400 kb. The whole cell lysate was precleared by incubation with 25 μL Gamma Bind G Sepharose beads (Pierce, USA) for 2 h at 4°C. The precleared lysate was incubated overnight at 4°C with 2 µg anti-hnRNP L antibody or 2 µg control IgG antibody. Next, 25 µL Gamma Bind G Sepharose beads were added to the lysate-antibody mixture and incubated for 2 h at 4°C. After washing the beads five times with high salt buffer and once with TE buffer, the RNA-protein (hnRNP L) complex was eluted in the elution buffer. The RNA-protein complex was de-crosslinked by 5 M NaCl at 65 °C for 2 h followed by RNA isolation using TRIzol reagent.

Actin staining

Stress fibers were observed by staining cellular F-actin using 5-TAMRA-Phalloidin (BACHEM, product number: 4095644). Control and MANCR-depleted BrCa cells grown in glass coverslips were fixed using freshly made 4% paraformaldehyde (PRILLS, Electron Microscopy Sciences) for 15 min at room temperature, washed three times (5 min each) in $1 \times PBS$ pH: 7.2 and permeabilized in 0.5% Triton-X-100 (in $1 \times PBS$) for 10 min on ice. Cells were then washed thrice in $1 \times$ PBS containing 1% Normal Goat serum (NGS), prior to incubating them with 5-TAMRA-Phalloidin (1:40,000 dilution of the stock in $1 \times PBS$ with NGS) for 30 min at room temperature. Cells were washed thrice in 1× PBS, stained with DAPI (5 min at room temperature), and then mounted using Vectashield (Vector laboratories Inc.) antifade mounting medium. The images were acquired in Axioimager Z1 (Zeiss) microscope using $63 \times 1.4 \, \text{NA}$ objective lens.

Acknowledgments

We thank members of the KVP and SGP laboratories for their valuable comments. We thank Prof. William Brieher (UIUC) for sharing reagents and for his valuable comments; Prof. Kirsten Lynch (UPenn) for hnRNP L shRNA constructs; Dr Ashish Lal (NCI) for dCas9-SIM3 vector; Drs Qinyu Hao (UIUC), Seyedsasan Hashemikhabir (IUPUI) and Prof. Sarath Chandra Janga (IUPUI) for initiating some of the experimental and bioinformatic analyses. We acknowledge the support from CCIL Tumor Engineering and Phenotyping Shared Resource, and Roy J. Carver Biotech Center (RNA sequencing).

Author Contributions

DKS and KVP designed the study. DKS, ZC and YJS performed most of the experiments. RC LMJ performed and analyzed RNA-pull down and Mass-spectrometry. DL and SGP performed and analyzed BrDu-PI flow cytometry analyses. YW and ERN performed and analyzed xenograft. RP performed actin-phalloidin staining. RKC, SM and KVB performed MANCR-sensitive hotspot analysis and ChIP-seq enrichment analysis and visualization. OG analyzed TCGA data set for NET1 expression in BrCa samples. AM performed chromatin fractionation and RT-qPCR. MA generated some of the stable cell lines. RB supervised the standardization of 3D BrCa culture. KVP supervised the project. DKS and KVP wrote the manuscript. All the authors read and agreed on the publication of the manuscript.

Contacts for Reagent and Resource Sharing

Requests for reagents and published resources should be directed to Kannanganattu V. Prasanth (kumarp@illinois.edu).

Disclosure Statement

No potential conflict of interest was reported by the authors.

Funding

This work was supported by National Institute of Health R21-AG065748 & R01-GM132458 to KVP, GM125196 to SGP, R00-HG010362 to KVB, R01-CA234025 to ERN, Department of Defense Era of Hope Scholar Award BC200206/W81XWH-20-BCRP-EOHS (ERN), Cancer Center at Illinois Seed Grants and Prairie Dragon Paddlers to KVP, National Science Foundation (NSF) to KVP [2243257; NSF Science and Technology Center for Quantitative Cell Biology] and SGP [1243372, 1818286, 2225264].

ORCID

Supriya G. Prasanth http://orcid.org/0000-0002-3735-7498 Kannanganattu V. Prasanth http://orcid.org/0000-0003-4587-8362

Data Availability Statement

The RNA-sequencing data from this study has been deposited to the GEO with the accession number GSE257538.

References

- Parker JS, Mullins M, Cheang MC, Leung S, Voduc D, Vickery T, Davies S, Fauron C, He X, Hu Z, et al. Supervised risk predictor of breast cancer based on intrinsic subtypes. J Clin Oncol. 2009;27: 1160–1167. doi:10.1200/JCO.2008.18.1370.
- Cable J, Heard E, Hirose T, Prasanth KV, Chen LL, Henninger JE, Quinodoz SA, Spector DL, Diermeier SD, Porman AM, et al. Noncoding RNAs: biology and applications-a Keystone Symposia report. Ann N Y Acad Sci. 2021;1506:118–141. doi:10.1111/nyas. 14713
- Zhang X, Meyerson M. Illuminating the noncoding genome in cancer. Nat Cancer. 2020;1:864–872. doi:10.1038/s43018-020-00114-3.
- Zhang W, Guan X, Tang J. The long non-coding RNA landscape in triple-negative breast cancer. Cell Prolif. 2021;54:e12966. doi:10. 1111/cpr.12966.
- Mattick JS, Amaral PP, Carninci P, Carpenter S, Chang HY, Chen LL, Chen R, Dean C, Dinger ME, Fitzgerald KA, et al. Long noncoding RNAs: definitions, functions, challenges and

- recommendations. Nat Rev Mol Cell Biol. 2023;24:430–447. doi:10. 1038/s41580-022-00566-8.
- Das PK, Siddika A, Rashel KM, Auwal A, Soha K, Rahman MA, Pillai S, Islam F. Roles of long noncoding RNA in triple-negative breast cancer. Cancer Med. 2023;12:20365–20379. doi:10.1002/cam4. 6600.
- Raju GSR, Pavitra E, Bandaru SS, Varaprasad GL, Nagaraju GP, Malla RR, Huh YS, Han YK. HOTAIR: a potential metastatic, drugresistant and prognostic regulator of breast cancer. Mol Cancer. 2023;22:65. doi:10.1186/s12943-023-01765-3.
- Jadaliha M, Zong X, Malakar P, Ray T, Singh DK, Freier SM, Jensen T, Prasanth SG, Karni R, Ray PS, et al. Functional and prognostic significance of long non-coding RNA MALAT1 as a metastasis driver in ER negative lymph node negative breast cancer. Oncotarget. 2016;7:40418–40436. doi:10.18632/oncotarget.9622.
- Arun G, Diermeier S, Akerman M, Chang KC, Wilkinson JE, Hearn S, Kim Y, MacLeod AR, Krainer AR, Norton L, et al. Differentiation of mammary tumors and reduction in metastasis upon Malat1 IncRNA loss. Genes Dev. 2016;30:34–51. doi:10.1101/gad.270959. 115.
- Jadaliha M, Gholamalamdari O, Tang W, Zhang Y, Petracovici A, Hao Q, Tariq A, Kim TG, Holton SE, Singh DK, et al. A natural antisense IncRNA controls breast cancer progression by promoting tumor suppressor gene mRNA stability. PLoS Genet. 2018;14: e1007802. doi:10.1371/journal.pgen.1007802.
- Tariq A, Hao Q, Sun Q, Singh DK, Jadaliha M, Zhang Y, Chetlangia N, Ma J, Holton SE, Bhargava R, et al. LncRNA-mediated regulation of SOX9 expression in basal subtype breast cancer cells. RNA. 2020;26:175–185. doi:10.1261/rna.073254.119.
- Diermeier SD, Chang KC, Freier SM, Song J, El Demerdash O, Krasnitz A, Rigo F, Bennett CF, Spector DL. Mammary tumor-associated RNAs impact tumor cell proliferation, invasion, and migration. Cell Rep. 2016;17:261–274. doi:10.1016/j.celrep.2016.08.081.
- Chang KC, Diermeier SD, Yu AT, Brine LD, Russo S, Bhatia S, Alsudani H, Kostroff K, Bhuiya T, Brogi E, et al. MaTAR25 IncRNA regulates the Tensin1 gene to impact breast cancer progression. Nat Commun. 2020;11:6438. doi:10.1038/s41467-020-20207-y.
- Pampaloni F, Reynaud EG, Stelzer EH. The third dimension bridges the gap between cell culture and live tissue. Nat Rev Mol Cell Biol. 2007;8:839–845. doi:10.1038/nrm2236.
- Tutty MA, Holmes S, Prina-Mello A. Cancer cell culture: the basics and two-dimensional cultures. Methods Mol Biol. 2023;2645:3–40. doi:10.1007/978-1-0716-3056-3_1.
- Katt ME, Placone AL, Wong AD, Xu ZS, Searson PC. In vitro tumor models: advantages, disadvantages, variables, and selecting the right platform. Front Bioeng Biotechnol. 2016;4:12. doi:10.3389/ fbioe.2016.00012.
- Jensen C, Teng Y. Is it time to start transitioning from 2D to 3D cell culture? Front Mol Biosci. 2020;7:33. doi:10.3389/fmolb.2020. 00033.
- Acker H, Carlsson J, Durand R, Sutherland RM, editors. Spheroids in cancer research. Methods and perspectives. Recent results in cancer research. Vol. 95. Berlin: Springer-Verlag; 1984. p. 1–183. doi:10.1007/978-3-642-82340-4.
- Tracy KM, Tye CE, Page NA, Fritz AJ, Stein JL, Lian JB, Stein GS. Selective expression of long non-coding RNAs in a breast cancer cell progression model. J Cell Physiol. 2018;233:1291–1299. doi:10. 1002/jcp.25997.
- Tracy KM, Tye CE, Ghule PN, Malaby HLH, Stumpff J, Stein JL, Stein GS, Lian JB. Mitotically-associated IncRNA (MANCR) affects genomic stability and cell division in aggressive breast cancer. Mol Cancer Res. 2018;16:587–598. doi:10.1158/1541-7786.MCR-17-0548.
- Wen S, Zeng M, Li Y, Hu X, Li S, Liang X, Zhu L, Yang S. Downregulation of MANCR inhibits cancer cell proliferation in mantle cell lymphoma possibly by interacting with RUNX2. Acta Biochim Biophys Sin (Shanghai). 2019;51:1142–1147. doi:10.1093/ abbs/gmz114.
- 22. Zhang X, Li H, Mao M, Wang X, Zheng J, Yang S. Mitotically-associated long non-coding RNA promotes cancer cell proliferation in

- hepatocellular carcinoma by downregulating miR-122a. Oncol Lett. 2019;18:6237-6242. doi:10.3892/ol.2019.10947.
- 23. Nagasawa M, Tomimatsu K, Terada K, Kondo K, Miyazaki K, Miyazaki M, Motooka D, Okuzaki D, Yoshida T, Kageyama S, et al. Long non-coding RNA MANCR is a target of BET bromodomain protein BRD4 and plays a critical role in cellular migration and invasion abilities of prostate cancer. Biochem Biophys Res Commun. 2020;526:128-134. doi:10.1016/j.bbrc.2020.03.043.
- 24. Huang NS, Lei BW, Tan LC, Yu PC, Shi X, Wang Y, Ji QH, Wei WJ, Lu ZW, Wang YL. Mitotically associated long non-coding RNA is a tumor promoter in anaplastic thyroid cancer. Ann Transl Med. 2020;8:1226-1226. doi:10.21037/atm-20-4530.
- Liu C, Li H, Li X, Zhao X, Zhang X. LncRNA MANCR positively affects the malignant progression of lung adenocarcinoma. BMC Pulm Med. 2021;21:272. doi:10.1186/s12890-021-01635-y.
- Tracy KM, Prior S, Trowbridge WT, Boyd JR, Ghule PN, Frietze S, 26. Stein JL, Stein GS, Lian JB. Bromodomain proteins epigenetically regulate the mitotically associated IncRNA MANCR in triple negative breast cancer cells. Crit Rev Eukaryot Gene Expr. 2024;34:61-71. doi:10.1615/CritRevEukaryotGeneExpr.2023050109.
- Dawson PJ, Wolman SR, Tait L, Heppner GH, Miller FR. MCF10AT: a model for the evolution of cancer from proliferative breast disease. Am J Pathol. 1996;148:313-319.
- Santner SJ, Dawson PJ, Tait L, Soule HD, Eliason J, Mohamed AN, 28. Wolman SR, Heppner GH, Miller FR. Malignant MCF10CA1 cell lines derived from premalignant human breast epithelial MCF10AT cells. Breast Cancer Res Treat. 2001;65:101–110. doi:10.1023/ a:1006461422273.
- Singh DK, Gholamalamdari O, Jadaliha M, Ling Li X, Lin YC, Zhang Y, Guang S, Hashemikhabir S, Tiwari S, Zhu YJ, et al. PSIP1/p75 promotes tumorigenicity in breast cancer cells by promoting the transcription of cell cycle genes. Carcinogenesis. 2017;38:966–975. doi:10.1093/carcin/bgx062.
- Lee KJ, Piett CG, Andrews JF, Mann E, Nagel ZD, Gassman NR. Defective base excision repair in the response to DNA damaging agents in triple negative breast cancer. PLoS One. 2019;14: e0223725. doi:10.1371/journal.pone.0223725.
- Lee KJ, Mann E, Wright G, Piett CG, Nagel ZD, Gassman NR. Exploiting DNA repair defects in triple negative breast cancer to improve cell killing. Ther Adv Med Oncol. 2020;12: 1758835920958354. doi:10.1177/1758835920958354.
- Alerasool N, Segal D, Lee H, Taipale M. An efficient KRAB domain 32. for CRISPRi applications in human cells. Nat Methods. 2020;17: 1093-1096. doi:10.1038/s41592-020-0966-x.
- 33. Krause M, Gautreau A. Steering cell migration: lamellipodium dynamics and the regulation of directional persistence. Nat Rev Mol Cell Biol. 2014;15:577-590. doi:10.1038/nrm3861.
- Tojkander S, Gateva G, Lappalainen P. Actin stress fibers-assembly, dynamics and biological roles. J Cell Sci. 2012;125:1855-1864. doi: 10.1242/jcs.098087.
- Herman IM, Crisona NJ, Pollard TD. Relation between cell activity and the distribution of cytoplasmic actin and myosin. J Cell Biol. 1981;90:84-91. doi:10.1083/jcb.90.1.84.
- Statello L, Guo CJ, Chen LL, Huarte M. Gene regulation by long non-coding RNAs and its biological functions. Nat Rev Mol Cell Biol. 2021;22:96-118. doi:10.1038/s41580-020-00315-9.
- 37. Sun Q, Hao Q, Prasanth KV. Nuclear long noncoding RNAs: key regulators of gene expression. Trends Genet. 2018;34:142-157. doi: 10.1016/j.tig.2017.11.005.
- Werner MS, Sullivan MA, Shah RN, Nadadur RD, Grzybowski AT, Galat V, Moskowitz IP, Ruthenburg AJ. Chromatin-enriched IncRNAs can act as cell-type specific activators of proximal gene transcription. Nat Struct Mol Biol. 2017;24:596-603. doi:10.1038/ nsmb.3424.
- Song EH, Oh W, Ulu A, Carr HS, Zuo Y, Frost JA. Acetylation of the RhoA GEF Net1A controls its subcellular localization and activity. J Cell Sci. 2015;128:913–922. doi:10.1242/jcs.158121.
- Qin H, Carr HS, Wu X, Muallem D, Tran NH, Frost JA. Characterization of the biochemical and transforming properties of

- the neuroepithelial transforming protein 1. J Biol Chem. 2005;280: 7603-7613. doi:10.1074/jbc.M412141200.
- 41. Menon S, Oh W, Carr HS, Frost JA. Rho GTPase-independent regulation of mitotic progression by the RhoGEF Net1. Mol Biol Cell. 2013;24:2655-2667. doi:10.1091/mbc.E13-01-0061.
- Murray D, Horgan G, Macmathuna P, Doran P. NET1-mediated RhoA activation facilitates lysophosphatidic acid-induced cell migration and invasion in gastric cancer. Br J Cancer. 2008;99: 1322-1329. doi:10.1038/sj.bjc.6604688.
- Carr HS, Zuo Y, Oh W, Frost JA. Regulation of focal adhesion kinase activation, breast cancer cell motility, and amoeboid invasion by the RhoA guanine nucleotide exchange factor Net1. Mol Cell Biol. 2013;33:2773-2786. doi:10.1128/MCB.00175-13.
- Zuo Y, Ulu A, Chang JT, Frost JA. Contributions of the RhoA guanine nucleotide exchange factor Net1 to polyoma middle T antigen-mediated mammary gland tumorigenesis and metastasis. Breast Cancer Res. 2018;20:41. doi:10.1186/s13058-018-0966-2.
- Oh W. Frost JA. Rho GTPase independent regulation of ATM activation and cell survival by the RhoGEF Net1A. Cell Cycle. 2014;13: 2765-2772. doi:10.4161/15384101.2015.945865.
- Ecimovic P, Murray D, Doran P, Buggy DJ. Propofol and bupivacaine in breast cancer cell function in vitro—role of the NET1 gene. Anticancer Res. 2014;34:1321-1331.
- Leyden J, Murray D, Moss A, Arumuguma M, Doyle E, McEntee G, O'Keane C, Doran P, MacMathuna P. Net1 and Myeov: computationally identified mediators of gastric cancer. Br J Cancer. 2006;94: 1204-1212. doi:10.1038/sj.bjc.6603054.
- Carr HS, Cai C, Keinänen K, Frost JA. Interaction of the RhoA exchange factor Net1 with discs large homolog 1 protects it from proteasome-mediated degradation and potentiates Net1 activity. J Biol Chem. 2009;284:24269-24280. doi:10.1074/jbc.M109.029439.
- Nakaya Y, Sukowati EW, Wu Y, Sheng G. RhoA and microtubule dynamics control cell-basement membrane interaction in EMT during gastrulation. Nat Cell Biol. 2008;10:765-775. doi:10.1038/ nch1739.
- Zou Z, Ohta T, Miura F, Oki S. ChIP-Atlas 2021 update: a data-mining suite for exploring epigenomic landscapes by fully integrating ChIP-seq, ATAC-seq and Bisulfite-seq data. Nucleic Acids Res. 2022; 50:W175-W182. doi:10.1093/nar/gkac199.
- Rothrock CR, House AE, Lynch KW. HnRNP L represses exon splicing via a regulated exonic splicing silencer. EMBO J. 2005;24:2792-2802. doi:10.1038/sj.emboj.7600745.
- Motta-Mena LB, Heyd F, Lynch KW. Context-dependent regulatory mechanism of the splicing factor hnRNP L. Mol Cell. 2010;37:223-234. doi:10.1016/j.molcel.2009.12.027.
- Hui J, Stangl K, Lane WS, Bindereif A. HnRNP L stimulates splicing of the eNOS gene by binding to variable-length CA repeats. Nat Struct Biol. 2003;10:33-37. doi:10.1038/nsb875.
- Shankarling G, Cole BS, Mallory MJ, Lynch KW. Transcriptome-wide RNA interaction profiling reveals physical and functional targets of hnRNP L in human T cells. Mol Cell Biol. 2014;34:71-83. doi:10. 1128/MCB.00740-13.
- 55. Liu Y, Sharma S, Watabe K. Roles of IncRNA in breast cancer. Front Biosci (Schol Ed). 2015;7:94-108. doi:10.2741/S427.
- 56. Mondal P, Meeran SM. Long non-coding RNAs in breast cancer metastasis. Noncoding RNA Res. 2020;5:208-218. doi:10.1016/j. ncrna.2020.11.004.
- Liu L, Zhang Y, Lu J. The roles of long noncoding RNAs in breast cancer metastasis. Cell Death Dis. 2020;11:749. doi:10.1038/s41419-
- Han YJ, Zhang J, Lee JH, Mason JM, Karginova O, Yoshimatsu TF, Hao Q, Hurley I, Brunet LP, Prat A, et al. The BRCA1 pseudogene negatively regulates antitumor responses through inhibition of innate immune defense mechanisms. Cancer Res. 2021;81:1540-1551. doi:10.1158/0008-5472.CAN-20-1959.
- Jin J, Tao Z, Cao J, Li T, Hu X. DNA damage response inhibitors: an avenue for TNBC treatment. Biochim Biophys Acta Rev Cancer. 2021;1875:188521. doi:10.1016/j.bbcan.2021.188521.
- Wang N, Gu Y, Chi J, Liu X, Xiong Y, Zhong C, Wang F, Wang X, Li L. Screening of DNA damage repair genes involved in the

- prognosis of triple-negative breast cancer patients based on bioinformatics. Front Genet. 2021;12:721873. doi:10.3389/fgene.2021.
- 61. Dubash AD, Guilluy C, Srougi MC, Boulter E, Burridge K, García-Mata R. The small GTPase RhoA localizes to the nucleus and is activated by Net1 and DNA damage signals. PLoS One. 2011;6: e17380. doi:10.1371/journal.pone.0017380.
- Srougi MC, Burridge K. The nuclear guanine nucleotide exchange 62. factors Ect2 and Net1 regulate RhoB-mediated cell death after DNA damage. PLoS One. 2011;6:e17108. doi:10.1371/journal.pone.
- 63. Herman AB, Tsitsipatis D, Gorospe M. Integrated IncRNA function upon genomic and epigenomic regulation. Mol Cell. 2022;82:2252-2266. doi:10.1016/j.molcel.2022.05.027.
- Quinn JJ, Chang HY. Unique features of long non-coding RNA biogenesis and function. Nat Rev Genet. 2016;17:47-62. doi:10.1038/ nra.2015.10.
- Ransohoff JD, Wei Y, Khavari PA. The functions and unique features of long intergenic non-coding RNA. Nat Rev Mol Cell Biol. 2018;19:143-157. doi:10.1038/nrm.2017.104.
- Singh DK, Prasanth KV. Functional insights into the role of nuclearretained long noncoding RNAs in gene expression control in mammalian cells. Chromosome Res. 2013;21:695-711. doi:10.1007/ s10577-013-9391-7.
- Papadimitriou E, Vasilaki E, Vorvis C, Iliopoulos D, Moustakas A, 67. Kardassis D, Stournaras C. Differential regulation of the two RhoAspecific GEF isoforms Net1/Net1A by TGF-beta and miR-24: role in epithelial-to-mesenchymal transition. Oncogene. 2012;31:2862-2875. doi:10.1038/onc.2011.457.
- Dutertre M, Gratadou L, Dardenne E, Germann S, Samaan S, Lidereau R, Driouch K, de la Grange P, Auboeuf D. Estrogen regulation and physiopathologic significance of alternative promoters in breast cancer. Cancer Res. 2010;70:3760-3770. doi:10.1158/0008-5472.CAN-09-3988.
- Humphries B, Wang Z, Yang C. Rho GTPases: big players in breast cancer initiation, metastasis and therapeutic responses. Cells. 2020; 9:2167. doi:10.3390/cells9102167.
- Shen X, Li J, Hu PP, Waddell D, Zhang J, Wang XF. The activity of guanine exchange factor NET1 is essential for transforming growth factor-beta-mediated stress fiber formation. J Biol Chem. 2001;276: 15362-15368. doi:10.1074/jbc.M009534200.

- Gilcrease MZ, Kilpatrick SK, Woodward WA, Zhou X, Nicolas MM, Corley LJ, Fuller GN, Tucker SL, Diaz LK, Buchholz TA, et al. Coexpression of alpha6beta4 integrin and guanine nucleotide exchange factor Net1 identifies node-positive breast cancer patients at high risk for distant metastasis. Cancer Epidemiol Biomarkers Prev. 2009;18:80-86. doi:10.1158/1055-9965.EPI-08-0842.
- Carr HS, Morris CA, Menon S, Song EH, Frost JA. Rac1 controls the subcellular localization of the Rho guanine nucleotide exchange factor Net1A to regulate focal adhesion formation and cell spreading. Mol Cell Biol. 2013;33:622-634. doi:10.1128/MCB.00980-12.
- Pardali K, Moustakas A. Actions of TGF-beta as tumor suppressor and pro-metastatic factor in human cancer. Biochim Biophys Acta. 2007;1775:21-62. doi:10.1016/j.bbcan.2006.06.004.
- Bui NHB, Napoli M, Davis AJ, Abbas HA, Rajapakshe K, Coarfa C, Flores ER. Spatiotemporal regulation of DeltaNp63 by TGFbetaregulated miRNAs is essential for cancer metastasis. Cancer Res. 2020;80:2833-2847. doi:10.1158/0008-5472.CAN-19-2733.
- 75. Debnath J, Muthuswamy SK, Brugge JS. Morphogenesis and oncogenesis of MCF-10A mammary epithelial acini grown in threedimensional basement membrane cultures. Methods. 2003;30:256-268. doi:10.1016/s1046-2023(03)00032-x.
- 76. Hao Q, Liu M, Daulatabad SV, Gaffari S, Song YJ, Srivastava R, Bhaskar S, Moitra A, Mangan H, Tseng E, et al. Monoallelically expressed noncoding RNAs form nucleolar territories on NOR-containing chromosomes and regulate rRNA expression. Elife. 2024;13: e80684. doi:10.7554/eLife.80684.
- 77. Shen Z, Sathyan KM, Geng Y, Zheng R, Chakraborty A, Freeman B, Wang F, Prasanth KV, Prasanth SG. A WD-repeat protein stabilizes ORC binding to chromatin. Mol Cell. 2010;40:99-111. doi:10.1016/j. molcel.2010.09.021.
- 78. Nelczyk AT, Ma L, Gupta AD, Gamage HEV, McHenry MT, Henn MA, Kadiri M, Wang Y, Krawczynska N, Bendre S, et al. The nuclear receptor TLX (NR2E1) inhibits growth and progression of triplenegative breast cancer. Biochim Biophys Acta Mol Basis Dis. 2022; 1868:166515. doi:10.1016/j.bbadis.2022.166515.
- Cancer Genome Atlas N. Comprehensive molecular portraits of human breast tumours. Nature. 2012;490:61-70. doi:10.1038/
- 80. Shevchenko A, Tomas H, Havlis J, Olsen JV, Mann M. In-gel digestion for mass spectrometric characterization of proteins and proteomes. Nat Protoc. 2006;1:2856-2860. doi:10.1038/nprot.2006.468.